

RESEARCH ARTICLE

Characterization of neurological disease progression in a canine model of CLN5 neuronal ceroid lipofuscinosis

Elizabeth J. Meiman¹  | Grace Robinson Kick² | Cheryl A. Jensen² | Joan R. Coates¹ | Martin L. Katz² 

¹Department of Veterinary Medicine and Surgery, College of Veterinary Medicine, University of Missouri, Columbia, Missouri, USA

²Neurodegenerative Diseases Research Laboratory, University of Missouri, Columbia, Missouri, USA

Correspondence

Martin L. Katz, Mason Eye Institute, University of Missouri School of Medicine, One Hospital Drive, Columbia, MO 65212, USA.

Email: katzm@health.missouri.edu

Funding information

U.S. National Institutes of Health, Grant/Award Number: EY031674; BioNexus KC; University of Missouri Life Sciences Fellowship

Abstract

Golden Retriever dogs with a frameshift variant in *CLN5* (c.934_935delAG) suffer from a progressive neurodegenerative disorder analogous to the CLN5 form of neuronal ceroid lipofuscinosis (NCL). Five littermate puppies homozygous for the deletion allele were identified prior to the onset of disease signs. Studies were performed to characterize the onset and progression of the disease in these dogs. Neurological signs that included restlessness, unwillingness to cooperate with the handlers, and proprioceptive deficits first became apparent at approximately 12 months of age. The neurological signs progressed over time and by 21 to 23 months of age included general proprioceptive ataxia, menace response deficits, aggressive behaviors, cerebellar ataxia, intention tremors, decreased visual tracking, seizures, cognitive decline, and impaired prehension. Due to the severity of these signs, the dogs were euthanized between 21 and 23 months of age. Magnetic resonance imaging revealed pronounced progressive global brain atrophy with a more than sevenfold increase in the volume of the ventricular system between 9.5 and 22.5 months of age. Accompanying this atrophy were pronounced accumulations of autofluorescent inclusions throughout the brain and spinal cord. Ultrastructurally, the contents of these inclusions were found to consist primarily of membrane-like aggregates. Inclusions with similar fluorescence properties were present in cardiac muscle. Similar to other forms of NCL, the affected dogs had low plasma carnitine concentrations, suggesting impaired carnitine biosynthesis. These data on disease progression will be useful in future studies using the canine model for therapeutic intervention studies.

KEYWORDS

Batten disease, carnitine, hereditary disorder, lysosomal storage disease, neurodegeneration

This is an open access article under the terms of the [Creative Commons Attribution-NonCommercial-NoDerivs](https://creativecommons.org/licenses/by-nc-nd/4.0/) License, which permits use and distribution in any medium, provided the original work is properly cited, the use is non-commercial and no modifications or adaptations are made.

© 2022 The Authors. *Developmental Neurobiology* published by Wiley Periodicals LLC.

1 | INTRODUCTION

The neuronal ceroid lipofuscinoses (NCLs) are a group of lysosomal storage disorders associated with variants in at least 13 genes (Beck-Wödl et al., 2018; Butz et al., 2020). They are characterized by intracellular accumulation of autofluorescent storage bodies, progressive neurological signs, and neurodegeneration. The CLN5 form of NCL is associated with sequence variants in *CLN5* that encodes a lysosomal protein with no homology to any other known protein and whose function remains unclear (De Silva et al., 2015; Jules et al., 2017; Larkin et al., 2013; Lebrun et al., 2009; Leinonen et al., 2017; Mamo et al., 2012; Moharir et al., 2013; Schmiedt et al., 2010). In the majority of cases, onset of clinical signs occurs in children between 2 and 8 years of age, typically beginning with declines in cognitive, motor, and language function followed by seizures and progressive loss of vision (Holmberg et al., 2000; Simonati et al., 2017; Xin et al., 2010). Behavior disturbances and sleep alterations may also occur (Kirveskari et al., 2001; Simonati et al., 2017). Progressive brain atrophy is apparent in CLN5 disease patients and by end-stage disease includes extreme global atrophy and loss of neurons of the cerebral cortex and cerebellum, degeneration of the thalamus, hippocampus and brainstem, and loss of myelin (Autti et al., 1992; Haltia et al., 2001; Holmberg et al., 2000; Tyynelä et al., 1997, 2004).

Naturally occurring CLN5 disease has been identified in several dog breeds, Borderdale sheep, and Devon cattle (Frugier et al., 2008; Gilliam et al., 2015; Houweling et al., 2006; Kolichski et al., 2016; Melville et al., 2005). A two base pair deletion and frame shift variant in *CLN5* (c.934_935delAG) that predicts a truncated CLN5 lacking the 39 C-terminal amino acids was identified in Golden Retrievers with this disorder (Gilliam et al., 2015). A limited description of neurological disease progression was previously reported for several CLN5-affected companion dogs. Studies were undertaken to more thoroughly characterize the disease progression of canine CLN5 disease, with a goal of obtaining baseline data that could form a basis for assessing the efficacy of potential therapeutic interventions using this model.

2 | MATERIALS AND METHODS

2.1 | Animals

Five Golden Retriever puppy littermates homozygous for the *CLN5:c.934_935delAG* variant were evaluated in this study (Gilliam et al., 2015). Four of the dogs were female and one was male. The affected puppies were identified by genotyping a litter of puppies generated by breeding a pair of carriers.

Genotyping was performed as described previously (Gilliam et al., 2015). The affected females were designated V, W, X, and Y, and the male dog was designated Z. Microchips were implanted in each of the puppies to ensure correct identification. The dogs were maintained on a 12:12 daily light cycle in AALAC-accredited facilities at the University of Missouri—Columbia. They received routine husbandry and veterinary care and were socialized outside of their pens daily. The study was performed in accordance with the U.S. National Research Council Guide for the Care and Use of Laboratory Animals and was approved by the University of Missouri Animal Care and Use Committee.

2.2 | Diagnostic imaging

Three of the five dogs had brain magnetic resonance imaging (MRI) performed at multiple time points. Dogs Y and Z underwent MRI at approximately 9, 18, and 23 months of age. Dog X underwent MRI at approximately 9 and 18 months of age. The two remaining dogs had brain imaging performed at one time point: Dog W at 21 months of age and Dog V at 20 months of age. All imaging was performed under general anesthesia using a 3.0T Toshiba/Canon Titan scanner (Canon Medical Systems USA, Tustin, CA, USA) with an orthopedic multichannel speeder coil. Images were obtained using the following parameters: localizer, T2-weighted sagittal (T2W: TR 3028–3316 ms, TE 120 ms, slice thickness 2.5 mm, slice gap 2.8 mm, FOV 576–784 × 640–800 mm), T2W coronal (TR 3028–3461 ms, TE 120 ms, slice thickness 2.5 mm, slice gap 2.8 mm, FOV 576–768 × 640–940 mm), T2W transverse (TR 6837–8302 ms, TE 120 ms, slice thickness 3 mm, slice gap 3.3 mm, FOV 512–768 × 512–704 mm), and MPRAGE (TR 6.8 ms, TE 2.7 ms, slice thickness 1 mm, slice gap 0.5 mm, FOV 400 × 420 mm). Contrast studies were not performed.

Quantification of ventricular system and whole brain volumes was performed using Brainsight software (Rogue Research, Montreal, Quebec, Canada) on the MPRAGE sequence images. A threshold was applied to the images to isolate the ventricles. Seeds, which propagated to subsequent images, were placed in the threshold ventricle of the most rostral or caudal slice containing ventricle. The software automatically tracked the seeds in subsequent slices, and manual adjustments were made to ensure that the entire ventricular system was accurately selected. The software then assembled the selected region of interest into a three-dimensional image of the ventricular system and used this composite to calculate the total volume of the ventricles in mm³. This procedure was repeated for whole brain volumetric analyses, with the threshold and seeds applied to isolate and select the brain parenchyma.

TABLE 1 Summary of clinicopathologic tests

| Age (months) | Test | Dog(s) |
|--------------|-----------------------------------|---------------|
| ~7.0 | CBC, chemistry, troponin, UA | V, W, X, Y, Z |
| ~9.5 | CBC, chemistry, troponin | V, W, X, Y, Z |
| ~12.5 | CBC, chemistry, troponin, UA | V, W, X, Y, Z |
| ~16.5 | CBC, chemistry, troponin, UA, CSF | V, W, X, Y, Z |
| 19.9 | Fasted blood glucose | V, W, X, Y, Z |
| ~20.0 | CBC, chemistry, troponin, UA, CSF | V, W, X, Y, Z |
| 21.0 | Fasted blood glucose | W, X, Y, Z |
| 22.0 | CBC, chemistry, troponin, UA, CSF | W |
| 23.1 | CBC, chemistry, troponin, UA, CSF | X |
| 23.0 | Fasted blood glucose | Y |
| ~23.0 | CBC, chemistry, troponin, UA, CSF | Y, Z |

Abbreviations: CBC, complete blood count; CSF, cerebrospinal fluid; UA, urinalysis.

2.3 | Clinical neurologic examinations

Monthly neurologic examinations were performed on all dogs between 9 and 22 months of age. Starting at 22 months of age, the frequency of examination was increased to every 1–2 weeks. Signs of neurologic dysfunction were subjectively monitored by a standardized clinical neurologic examination (Lorenz et al., 2011). Components of the neurologic examination included observation of mentation, posture, and gait; testing of cranial nerves; evaluation of postural reactions (paw replacement, hopping, wheelbarrow, and extensor postural thrust); spinal reflexes (myotatic and flexor); and sensory testing. Gait evaluation was assessed as normal or abnormal with the presence of ataxia (cerebellar, general proprioceptive, vestibular) and paresis (ambulatory, nonambulatory). Postural reactions, spinal reflexes, cranial nerve tests, and sensation were assessed as intact, decreased, or absent. Dogs were evaluated for abnormal movement and seizure activity. The dogs also were evaluated for ability to prehend four meatballs from a pair of food dishes positioned in identical orientation and 10 feet away. At 16 months of age, the dogs became too agitated for handling, and the neurologic examination was modified. Modified neurologic assessments included mentation, posture and gait, and ability to prehend four meatballs. Age at onset was recorded for the following neurologic deficits: behavior changes, proprioceptive deficits, general proprioceptive ataxia, menace response deficits, aggressive behaviors, cerebellar ataxia and intention tremors, decreased visual tracking, seizure onset, cognitive decline, and abnormal prehension. Clinical findings were documented until humane euthanasia was performed. Pupillary light reflexes were assessed in Dogs W, X, Y, and Z at 21 months of age. Vision was assessed using a cotton ball tracking test as described previously (Gelatt et al., 2013; Kick et al., 2021; Skerritt, 2018). Each of the dogs was humanely euthanized at the point at which behavioral changes and refractory seizure activity put them

at high risk for injuring themselves and their handlers due to a combination of agitation, loss of coordination, and aggression.

2.4 | Clinicopathologic analyses

Clinicopathologic analyses were performed at various ages throughout disease progression in all dogs (Table 1). Dogs were fasted for approximately 12 h before sample collections. Blood was collected for complete blood count (CBC; EDTA-whole blood), chemistry panel, and cardiac troponin (lithium heparin-whole blood). For urinalysis, urine was collected by free catch during bladder expression under anesthesia. Cerebrospinal fluid (CSF) was collected from the cerebellomedullary cistern for immediate analysis.

2.5 | Plasma carnitine assay

Lithium heparinized whole blood samples were collected from Dogs X, Y, and Z at 22.3 months of age for plasma carnitine analysis. Blood samples were centrifuged at 3200 RPM (RCF 1545 × *g*; Unico PowerSpin MX, Dadyon, NJ, USA) for 10 min, and supernatant plasma was separated and frozen at –80°C. Frozen plasma samples were shipped on dry ice to the University of California San Diego Biochemical Genetics Laboratory for analysis.

Plasma free carnitine was assayed by stable-isotope dilution with 50 μM ²H₃-carnitine (methyl-d₃; Cambridge Isotope Laboratories, Tewksbury, MA, USA) after deproteinization with acetonitrile+0.1% formic acid (1:5; by volume), cooling for 10 min on ice and centrifugation at 17,136 × *g* and 5°C for 5 min. Plasma total carnitine was obtained by alkaline hydrolysis with 0.08 N potassium hydroxide after incubation for 15 min at 65°C, following neutralization with equal

TABLE 2 Ages at which dogs were euthanized

| Dog | Sex | Age at euthanasia (months) |
|-------|-----|----------------------------|
| Dog V | F | 20.1 |
| Dog W | F | 21.9 |
| Dog X | F | 23.1 |
| Dog Y | F | 23.4 |
| Dog Z | M | 23.4 |

equivalents of hydrochloric acid and then deproteinization, as above.

Carnitine was analyzed in the supernatant (5 μ l injection volume) by flow injection analysis (0.2 ml/minute of 60% acetonitrile+0.1% formic acid) in an API4000 triple quadrupole mass spectrometer (Sciex, Framingham, MA, USA) using the transitions m/z 161 (m/z 164, for d3-carnitine) to m/z 85, and m/z 103 for confirmation, using collision energies of 29 v and 23 v, respectively. Source parameters were collisionally activated dissociation 9, curtain gas 50, GS1 70, GS2 40, ion spray 5000 v, and temperature 200°C. Quantification was done against a calibration curve using 2, 12.5, 50, 75, and 150 μ M carnitine.

2.6 | Microscopic evaluations

The five dogs evaluated in this study were euthanized between 20 and 23.5 months of age (Table 2). Euthanasia was performed when the dogs' quality of life was assessed to be compromised due to high risk of injury as a result of loss of coordination and agitated behavior. Each euthanasia procedure was performed between 5 and 6 h after the onset of the light phase of the daily light cycle. The dogs were euthanized via intravenous infusion of pentobarbital (15 ml of 390 mg/ml pentobarbital Fatal-Plus solution, Dearborn, MI, USA). Tissue collections commenced immediately after euthanasia and were completed within 30 min. Tissues collected included the entire brain, cervical and thoracic spinal cord segments, and heart ventricular walls. Immediately after the brain was collected from each dog, it was immersed in ice-chilled PlasmaLyte (Baxter Healthcare, Deerfield, IL, USA) for 10 mins. The brain was then cut into 4 mm thick coronal slices using an Adult Rhesus monkey brain matrix (Electron Microscopy Sciences, Hatfield, PA, USA). Half of each brain slice was fixed in 2.0% glutaraldehyde, 1.12% paraformaldehyde, 130 mM sodium cacodylate, 1 mM CaCl₂, pH 7.4 (EM Fix) and the other half in 0.05% glutaraldehyde, 120 mM sodium cacodylate, 1 mM CaCl₂, pH 7.4 (Immuno Fix). Portions of the other tissues were preserved in each of the same fixatives.

Portions of the samples preserved with EM Fix were post-fixed in osmium tetroxide and embedded in epoxy resin (Katz et al., 2005). Sections of these samples were cut at a thick-

ness of 0.6 μ m for light microscopy and 70–90 nm for electron microscopy. Sections for light microscopic examination were stained with Toluidine blue, and sections for electron microscopic examination were mounted on thin-barred copper grids and stained with uranyl acetate and lead citrate. Light microscopy was performed using a Leica DMI 6000B microscope, and electron microscopy was performed using a JEOL JEM-1400 transmission electron microscope equipped with a Gatan digital camera.

A segment of each immuno-fixed sample was embedded in paraffin and sectioned at a thickness of 5 μ m. Sections were immunostained for localization of GFAP, Iba1, and LAMP2 as described previously (Kick et al., 2021; Morgan et al., 2013; Schmutz et al., 2019; Villani et al., 2019). A sample of each immuno-fixed tissue was washed in 170 mM sodium cacodylate, pH 7.4 and embedded in Tissue Tek cryo-embedding medium (Sakura FineTek, Torrance, CA, USA). Sections of the cryo-embedded samples were cut with a Microm HM525 cryostat (Thermo Scientific, Waltham, MA, USA) at a thickness of 8 μ m. The sections were mounted in 107 mM sodium cacodylate buffer on Superfrost Plus slides (Fisher Scientific, Waltham, MA, USA) and were examined for NCL storage body-specific autofluorescence as described previously (Katz & Redmond, 2001).

2.7 | Statistical analyses

All statistical tests were performed using SigmaPlot (Systat Software Inc., San Jose, CA). Normality was confirmed with the Shapiro–Wilk test and equal variance with the Brown–Forsythe test. Linear regression analysis was used to assess age-related changes in whole brain volumes, ventricular system volumes, and the ventricular system to whole brain volume ratios between 9.5 and 22.5 months of age.

3 | RESULTS

3.1 | MRI evaluations

Brain MRI at 9 months of age showed no significant abnormalities in the dogs except for lateral ventricle asymmetry in dog Z (Figure 1c). MRI at 18, 20, 21, and 23 months of age showed progressive diffuse brain atrophy, which included diffuse thinning of the cerebral cortex, blunted cerebral gyri, prominent widened sulci, increased prominence of cerebellar folia, and decrease in the size of the interthalamic adhesion (Figure 1). There was loss of gray and white matter distinction and decrease in distinction of striatum. Thinning was noted in the corpus callosum and internal capsule. Increase in CSF volume in the entire ventricular system became marked between 18 and 23 months of age (Figure 1d,e).

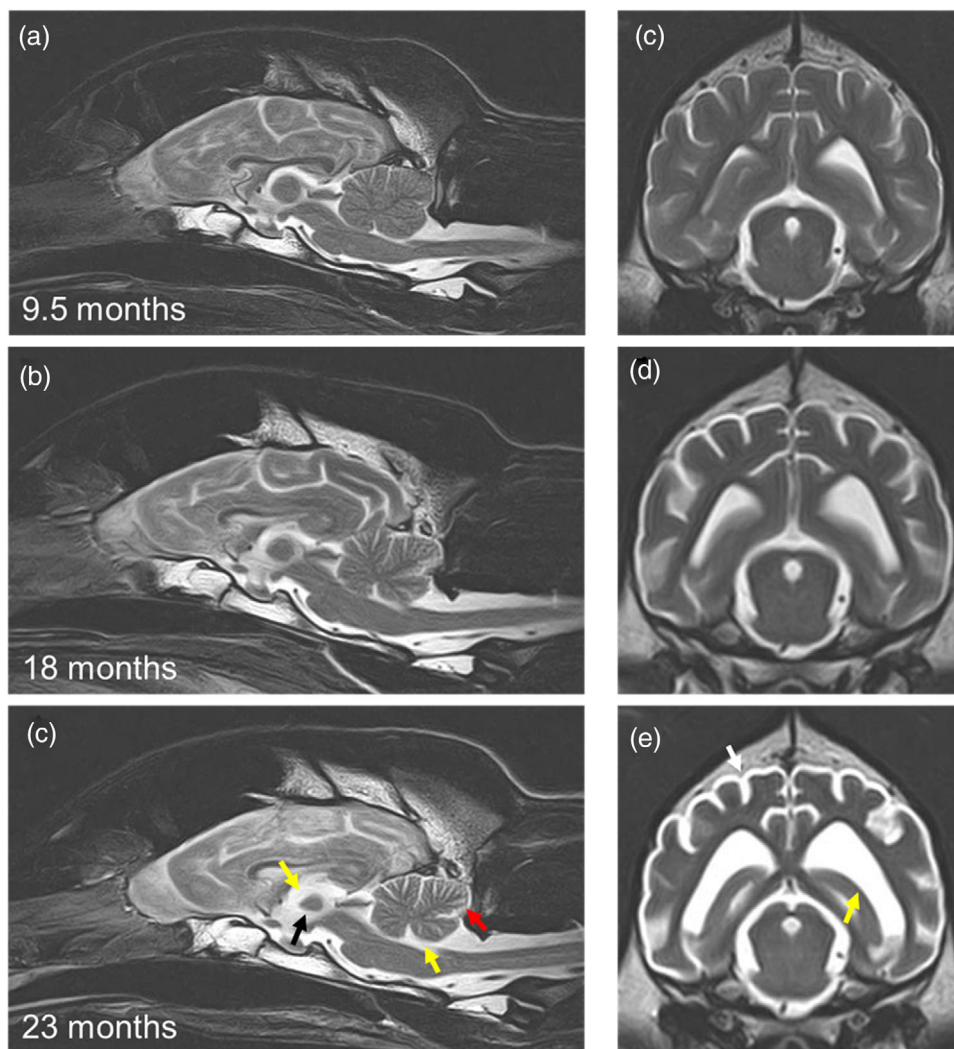


FIGURE 1 Magnetic resonance (MR) images from dog Z at 9.5 (a and c), 18 (b and d) and 23 (c and e) months of age show progressive diffuse brain atrophy evidenced by diffuse thinning of the cerebral cortex, blunted cerebral gyri and widened sulci (white arrow), prominent cerebellar folia (red arrow), and reduction of the size of the interthalamic adhesion (black arrow). Progressive enlargement of the ventricular system is also apparent (yellow arrows)

Quantitative analysis of three-dimensional reconstructions of the brain using MR images demonstrated profound progressive disease-related brain atrophy. Average whole brain volume decreased by approximately 24%, from 89,000 mm³ at 9.5 months of age (dogs X, Y, and Z) to 68,000 mm³ at 22.5 months of age (dogs W, Y, and Z) ($p < .001$) (Figure 2b). Over the same age range, the average volume of the ventricular system increased more than sevenfold ($p < .001$) (Figure 2a). The average ratio of ventricular to whole brain volume increased almost 10-fold ($p < .001$, Figure 2c).

3.2 | Neurologic signs

Onset of neurologic abnormalities occurred in all five dogs between 12.0 and 14.1 months of age. Initial manifestations

of disease included subtle behavior changes that were noted only at the time of neurologic examination: restlessness and unwillingness to cooperate with the examiner. Proprioceptive placement deficits were apparent in two of five dogs at this age. At approximately 15 months of age, some dogs displayed episodes of hyperactivity, and demeanor in one dog became increasingly timid and skittish. Four of five dogs exhibited proprioceptive placement deficits and in one dog general proprioceptive ataxia became apparent. At 16 months of age, the gait in all dogs showed mild general proprioceptive ataxia and their stance was wide based. In all dogs, menace response was inconsistent but visual tracking was normal. Temperament changes included resistance to handling, unruly body movements, and attempts to bite. After 16 months, the dogs became quite agitated during the neurologic examinations. Therefore, due to concerns of potential injuries to the examiners and the

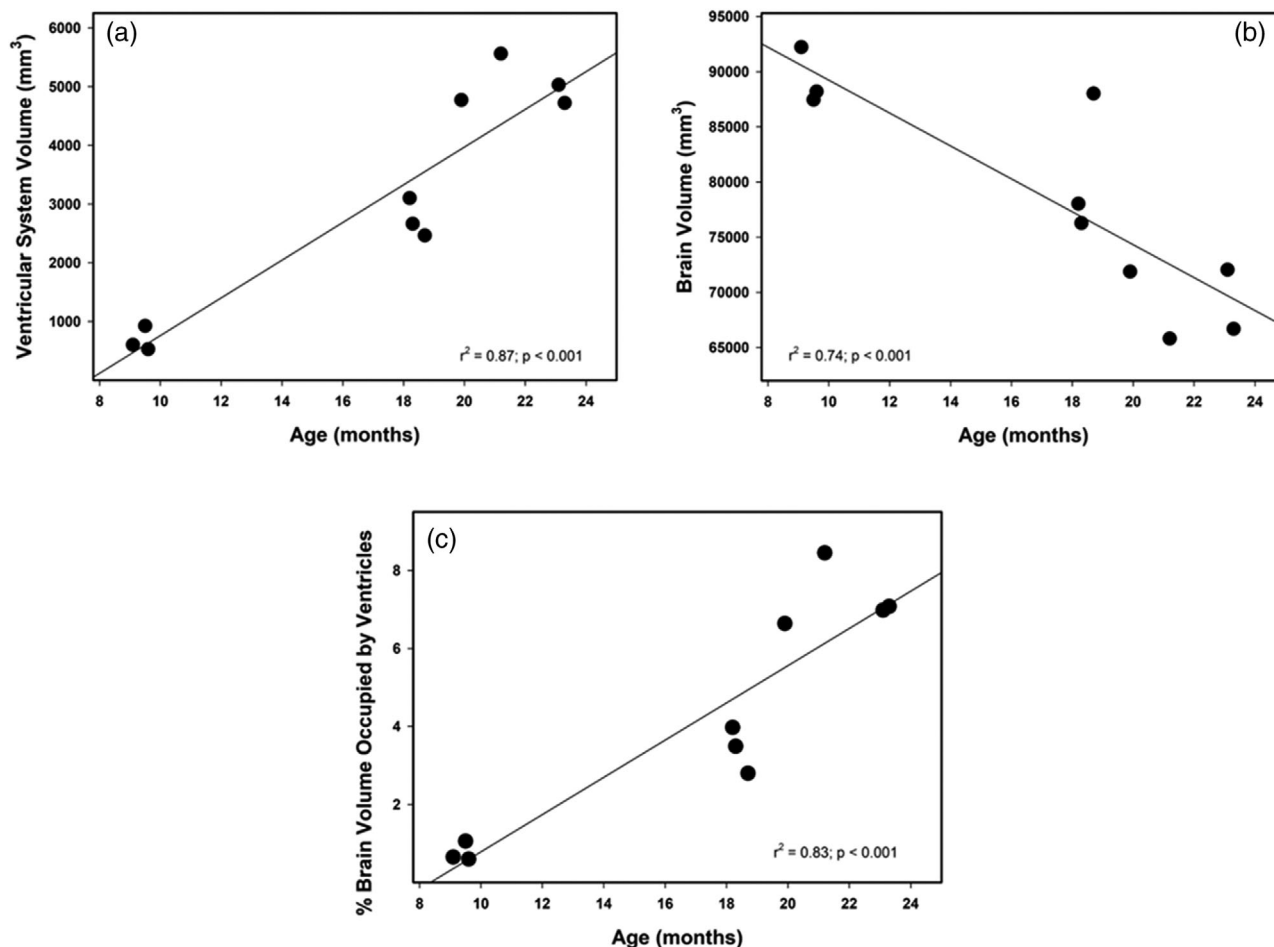


FIGURE 2 Between 9.5 and 22.5 months of age, the volume of the ventricular system (a) increased more than sevenfold, whole brain volume (b) decreased by approximately 24%, and the fraction of the brain volume represented by the ventricles (c) increased almost 10-fold. All age-related changes were statistically significant

dogs, the examinations were modified and abbreviated. At 17–19 months, the gait showed progressively severe general proprioceptive ataxia and onset of cerebellar ataxia. Posture showed wide base stance and subtle intention tremors involving the head. At 20 months of age, one dog exhibited food aggression behavior. At 21 months, visual deficits included decreased visual tracking and bumping into obstacles when navigating an unfamiliar area. Observed behavior changes at this point included increasingly skittish demeanor, overreactive responses to tactile stimuli (i.e., being petted or handled), and periodic aggression toward handlers. At 22 months of age, onset of fly-biting seizures and occasional focal myoclonic episodes involving the head and neck were apparent. Episodes were controlled with phenobarbital therapy. Cognitive decline was suspected in one dog due to lack of focus and difficulty completing previously learned examination tasks (locating and eating meatballs placed approximately 10 feet from the dog). By 23 months of age, two of the three dogs still alive showed decreases in prehension ability. The dogs were humanely euthanized due to more severe

TABLE 3 Approximate age at onset of neurologic disease signs in CLN5-affected Golden Retrievers

| | |
|---|--------------|
| Behavior changes | 12–14 months |
| Proprioceptive deficits | 12–16 months |
| General proprioceptive ataxia | 16 months |
| Menace response deficits | 16 months |
| Aggressive behaviors | 20 months |
| Cerebellar ataxia and intention tremors | 20 months |
| Decreased visual tracking | 21 months |
| Seizure onset | 22 months |
| Cognitive decline | 22–23 months |
| Abnormal prehension | 23 months |

mentation changes, aggressive behavior, loss of coordination, and myoclonic seizures. Neurologic signs and age of onset are summarized in Table 3. The progression of selected disease-related behavioral abnormalities and clinical signs are illustrated in Videos S1 and S2.

3.3 | Clinical-pathological findings

CBC remained normal throughout all routine diagnostic time points of this study. Serum chemistry profiles revealed elevated phosphorus levels (8.2–9.2 mg/dl, normal 2.3–5.0 mg/dl) in all dogs at the time of first diagnostic sample acquisition around 7 months of age, with gradual decreases over the following months. Phosphorus levels normalized in four of five dogs by approximately 20 months of age, while one dog had a persistently high level (5.6 mg/dl) through time of euthanasia at 23 months of age. These changes were consistent with normal age- and growth-related trends (von Dehn, 2014). Mild low total protein levels (5.2–5.3 g/dl, normal 5.4–6.9 g/dl) were also detected in four dogs at initial sample acquisition around 7 months of age and resolved by around 16 months of age. This was also considered an age-related finding (von Dehn, 2014). Creatine kinase levels were sporadically elevated (227–440 U/L, normal 40–226 U/L) in all five dogs over the course of the study. Plasma cardiac troponin concentrations remained within the reference range (0.00–0.05 ng/ml) for all five dogs from 7 to 23.4 months of age with one exception. In Dog X, the troponin concentration rose from 0.02 ng/ml at 20 months of age to 0.16 ng/ml at 23.1 months.

Elevated blood glucose levels were observed in all five dogs (125–200 mg/dl, normal 80–115 mg/dl), with onset at varying time points from 7 to 16 months of age and persisted at subsequent diagnostic time points over the dogs' lifespans. Due to suspicion that this represented a stress-induced hyperglycemia response occurring when the dogs were moved from their normal housing environment and anesthetized for diagnostic procedures prior to blood collection, isolated fasted blood glucose levels were taken at two timepoints (20 and 21 months of age) during weeks in which no anesthetic procedures were scheduled. These samples were taken in the dogs' home environment with minimal handling prior to sample collection to minimize exogenous stressors and were processed using the same analyzers as for all prior blood analyses. Isolated fasted blood glucose levels were within low to normal range (65–95 mg/dl, normal 80–115 mg/dl) in all dogs at each recheck. These data are consistent with the possibility that the elevations in blood glucose levels were normal physiologic responses to stress.

Routine urinalyses were largely unremarkable, except for the urine specific gravity often within the isosthenuric range (1.008–1.012). This was attributed to use of dexmedetomidine during anesthetic procedures and resultant diuresis (Villela et al., 2005), as well as maintenance intravenous fluid therapy administered during anesthetic procedures prior to urine sample collection. Results of CSF analysis were within reference ranges except an albuminocytologic dissociation in one dog at 16.5 months of age.

3.4 | Plasma carnitine analyses

In the three affected dogs that were evaluated, plasma carnitine existed primarily in the free form and as the acetyl ester (Table 4). C3–C18 fatty acid esters each represented only a minor fraction of the total plasma carnitine. In the affected dogs, mean plasma concentrations of both total and free carnitine were below the lower limit of the reference range for healthy dogs (Table 4). The mean ratio of esterified to free carnitine was slightly above the upper limit of the reference range.

3.5 | Microscopic evaluations

Neurons throughout the brain and spinal cord of all five dogs exhibited substantial accumulations of autofluorescent inclusions with fluorescence properties typical of the NCLs. In Figures 3 and 4 are representative micrographs showing these accumulations in cerebral cortex, deep cerebellar nucleus, and spinal cord. These inclusions are immunolabeled for the lysosomal membrane marker LAMP2 (Figure 5). Similar inclusions were present in most other regions of the brain as well as in the retina, as reported previously for the canine CLN5 disease (Gilliam et al., 2015; Kick et al., 2021; Kolicheski et al., 2016). Inclusions with similar autofluorescence properties were present in cardiac muscle fibers, primarily adjacent to the myocyte nuclei (Figure 6a). The inclusions closest to the nuclei immunolabeled for the lysosomal marker protein LAMP2 (Figure 6b). No autofluorescent inclusions were observed in cryostat sections of pancreas from any of the dogs.

The ultrastructure of the disease-specific cellular inclusions from brain and spinal cord was evaluated. In brain and spinal cord neurons, the contents of the storage bodies consisted primarily of tightly packed membrane-like structures (Figures 7 and 8). The arrangement of these structures varied, even within the same cell, from lamellar to vesicular. Most of the inclusions were between 1 and 6 μ m in diameter.

Activated microglia and astrocytes, detected via immunolabeling for Iba1 and GFAP, respectively, are indicators of neuroinflammation in many progressive neurodegenerative disorders (Carroll & Chesebro, 2019; Hampel et al., 2020; Kaur et al., 2019; Kovacs, 2018; Liberman et al., 2019; Linnerbauer & Rothhammer, 2020; Linnerbauer et al., 2020; Lynch, 2020; Stephenson et al., 2018; Wright-Jin & Gutmann, 2019), including NCL disorders (Bible et al., 2004; Groh et al., 2013, 2016; Katz et al., 2020; Kay & Palmer, 2013; Macauley et al., 2009; Mendsaikhan et al., 2019; Oswald et al., 2005; Pontikis et al., 2004; Xiong & Kielian, 2013). In the CLN5-affected Golden Retrievers, abundant activated microglia were present in the spinal cord gray matter, the cerebellar cortex, deep cerebellar nuclei, and throughout the cerebral cortex (Figure 9).

TABLE 4 Plasma carnitine concentrations for CLN5-affected Golden Retrievers

| | Plasma concentration (nmol/ml) | | | | |
|-------------------|--------------------------------|-------------|--------------|------------------|-----------------|
| | Total | Free | Acetyl ester | Total esterified | Esterified:free |
| Subject dogs* | 13.77 ± 3.15 | 9.32 ± 2.62 | 3.66 ± 0.47 | 4.44 ± 0.53 | 0.57 ± 0.14 |
| Reference values# | 17–43 | 17–38 | – | 0–23 | 0–0.54 |

*Values are mean ± SEM for three dogs.

#As determined by the UCSD Biochemical Genetics Laboratory.

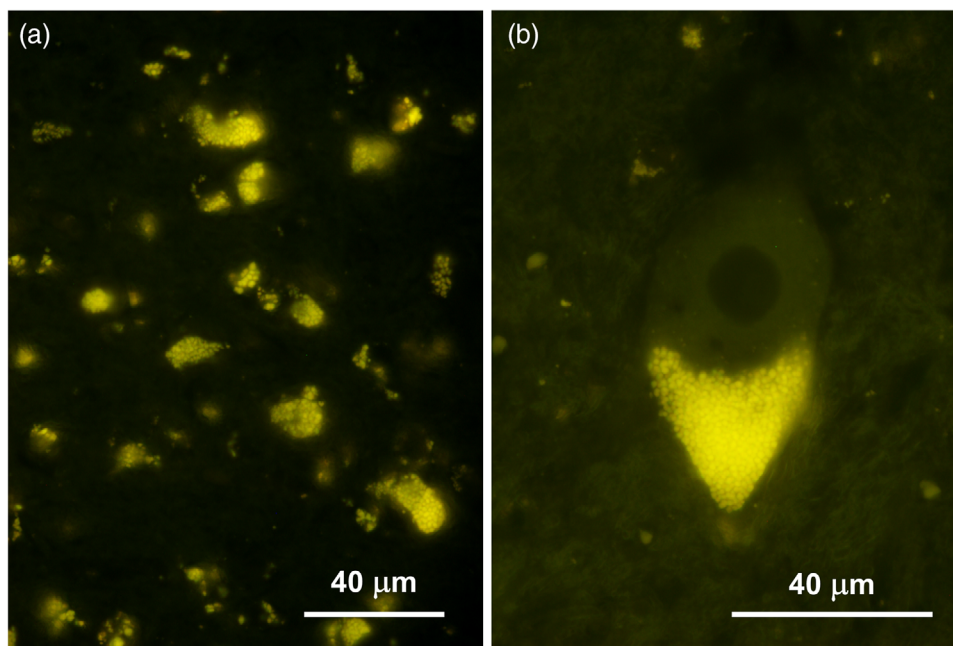


FIGURE 3 Fluorescence micrographs of unstained cryostat sections of cerebral cortex from dog V (a) and deep cerebellar nucleus from dog Y (b). Almost all neurons in both regions of the brain contained massive numbers of autofluorescent inclusions

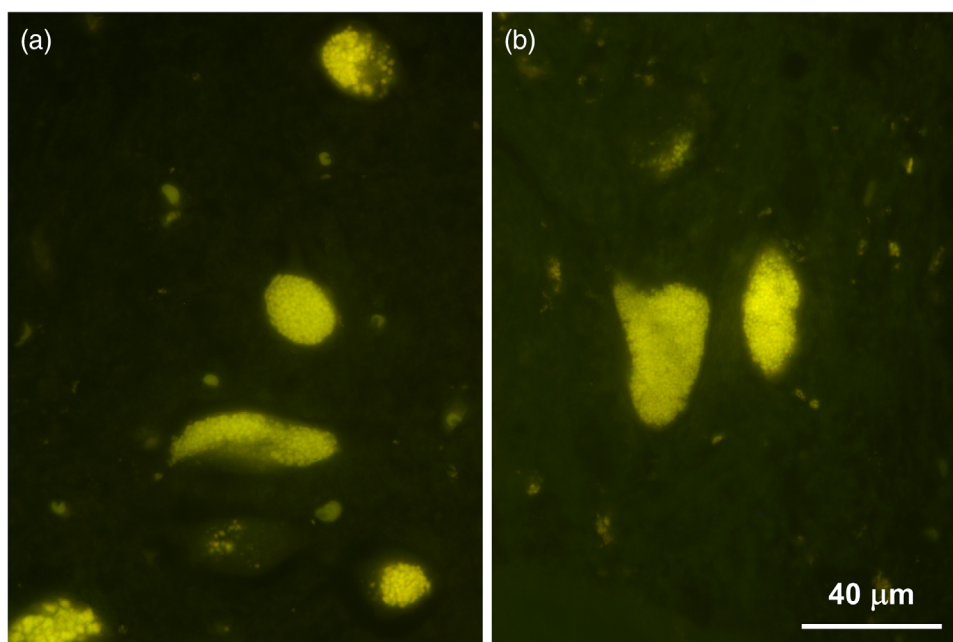


FIGURE 4 Fluorescence micrographs of unstained cryostat sections of cervical spinal cord from dog Y (a) and thoracic spinal cord from dog X (b). Images show substantial accumulations of autofluorescent inclusions in ventral horn neurons. Bar in (b) indicates magnification of both micrographs

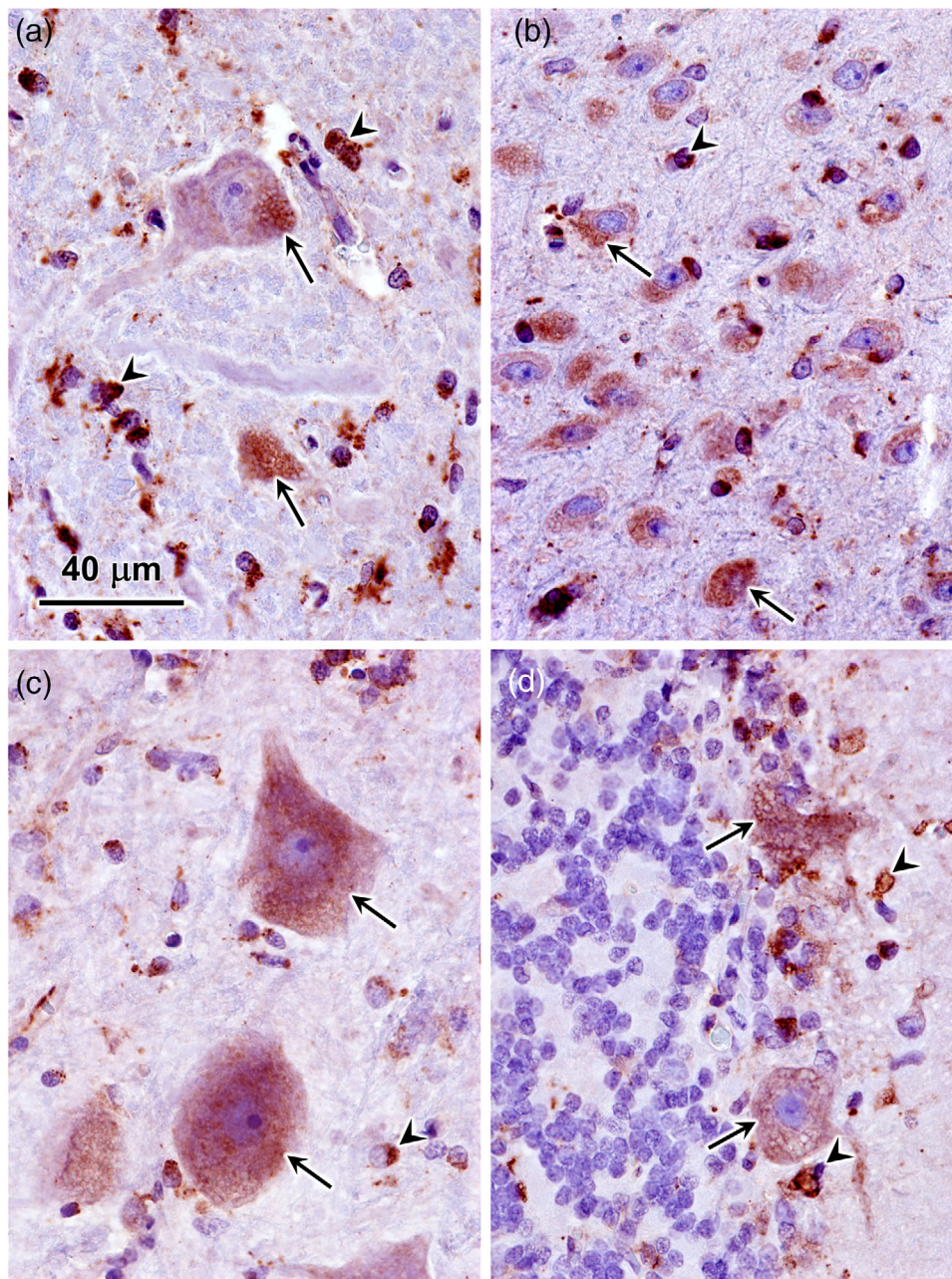


FIGURE 5 Paraffin sections of cervical spinal cord ventral horn (a), occipital cortex (b), deep cerebellar nucleus (c) and cerebellar cortex (d) from dog V immunolabeled for LAMP2 localization. Arrows indicate neurons with immunolabeled inclusions; arrowheads indicate glia with LAMP2 immunolabel. Bar in (a) indicates magnification of all four micrographs

Likewise, substantial numbers of activated astrocytes were present throughout the cerebellar cortex and cerebral cortex (Figure 10). Activated astrocytes were much less abundant in the deep cerebellar nuclei (Figure 10c) and were not observed in the spinal cord gray matter.

4 | DISCUSSION

Canine models have played significant roles in the development of therapeutic interventions for a number of hereditary

neurological disorders (Bockenbauer & Kleta, 2017; Fletcher & Taylor, 2016; King et al., 2017; Kondagari et al., 2015; Partridge & Rossmeisl, 2020; Topál et al., 2019). Among these is the CLN2 form of NCL. Preclinical studies of enzyme replacement therapy using a Dachshund model for this disorder led to the successful application of this approach for treating children with CLN2 disease (Katz et al., 2014; Lewis et al., 2019; Schaefer et al., 2021; Schulz et al., 2018; Vuilleminot et al., 2015; Whiting et al., 2014). The canine CLN2 disease model is also being used to investigate gene and stem cell-based approaches to treatment (Katz et al., 2015;

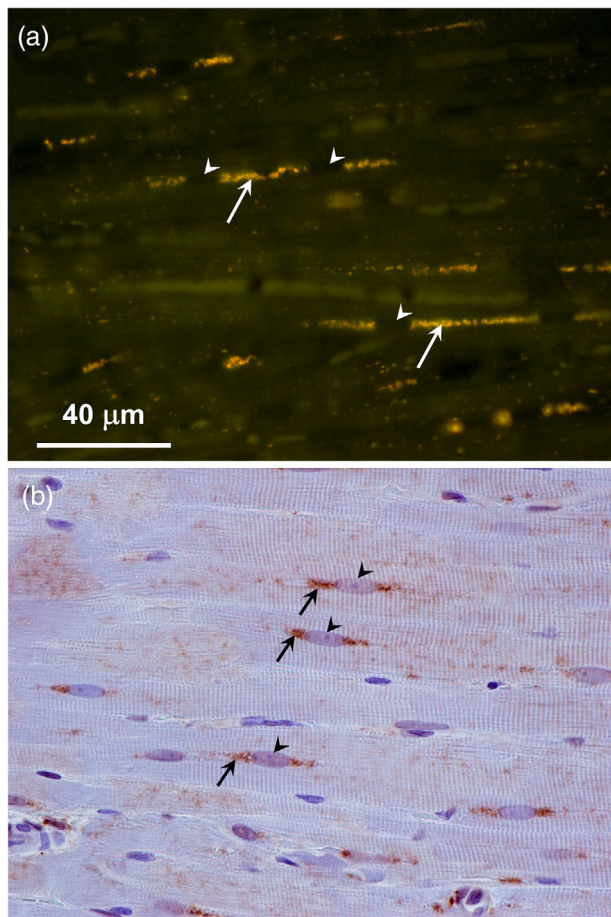


FIGURE 6 (a) Fluorescence micrograph of unstained cryostat section of heart ventricular wall muscle from dog X. Accumulations of autofluorescent inclusions were present along the muscle fibers (arrows). (b) Paraffin section of ventricular wall muscle from the same dog immunolabeled for LAMP2 localization (arrows). Arrowheads in both micrographs indicate the locations of muscle fiber cell nuclei

Katz, Johnson, et al., 2017; Tracy et al., 2016; Whiting et al., 2016). Like the TPP1 enzyme encoded by the *CLN2* (*TPPI*) gene, the *CLN5* protein has been shown to be trafficked to lysosomes (De Silva et al., 2015; Jules et al., 2017; Moharir et al., 2013). Therefore, it appears likely that *CLN5* disease will be amenable to similar approaches to therapy. The dog model described in this study could facilitate evaluation of these approaches to treatment and their adoption for treating children with this disorder. Semen from dogs with the *CLN5* disease variant suitable for use in breeding by artificial insemination has been preserved so that affected dogs can be produced for therapeutic intervention studies.

In addition to strong correlations at the molecular level (canine *CLN5* has 92% homology with human *CLN5*), the Golden Retrievers with the c.934_935delAG variant in *CLN5* recapitulate very well most clinical aspects of the human disease (Basak et al., 2021). Observed neurologic deficits manifest along similar timelines of disease relative

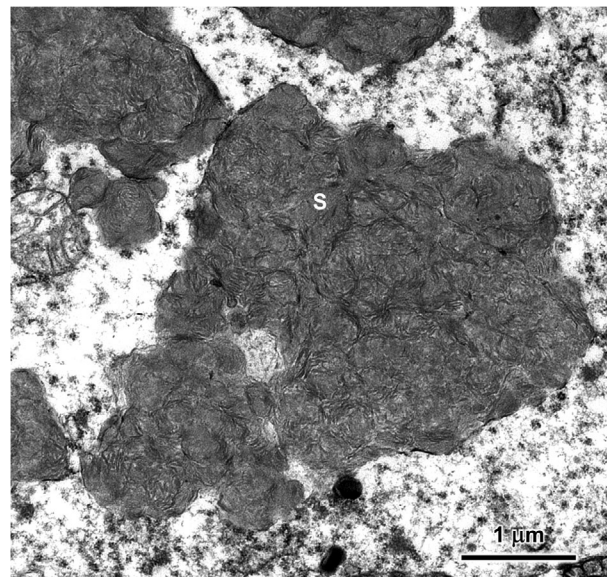


FIGURE 7 Electron micrograph of a disease-specific storage body in the perinuclear region of an occipital cortex neuron from dog X

to the human and dog lifespans, although direct comparison between humans and dogs with respect to age can be difficult. The affected dogs exhibit a robust disease phenotype, the features of which can be assessed to evaluate the efficacy of any potential therapeutic intervention within a reasonable timeframe. For example, the affected dogs exhibited proprioceptive ataxia as early as 16 months of age that progressed in severity over the next 5 to 7 months. Preservation of normal gait over this time period could be used as an objective indication of therapeutic efficacy. Other progressive behavioral and neurologic signs that could be used to assess the efficacy of therapeutic interventions include loss of visual tracking ability, loss of menace response, the development of aggressive behaviors, intention tremors, cognitive decline, and seizures. Quantitative measures have been developed for assessing the development and progression of some of these signs. For example, cognitive decline can be assessed by training the dogs to perform a task prior to the onset of disease signs and then evaluating the decline in performance as the disease progresses (Sanders et al., 2011). Test performance on cognitive tasks can be scored quantitatively, therefore lending utility in comparing cognition at different points along disease progression. This type of test could be useful in *CLN5* disease therapeutic intervention studies.

Brain atrophy, as assessed with quantitative volumetric MRI, is a robust noninvasive indicator of disease progression in the dog model that can be translated for human disease research and treatment applications (Löbel et al., 2016). In the affected dogs, brain ventricular volumes increased an average of over sevenfold and whole brain volume decreased an average of 23% between 9.5 and 22.5 months of age. This degree of brain atrophy likely underlies the development of most of

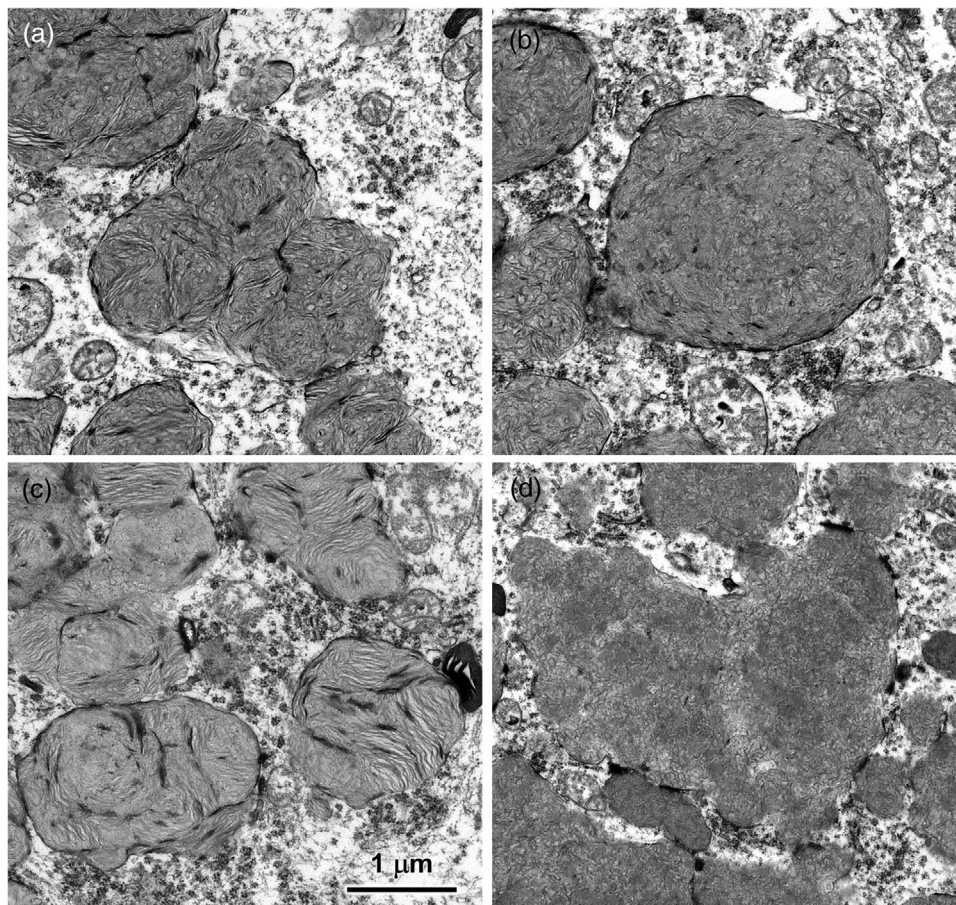


FIGURE 8 Electron micrographs of disease-specific storage bodies in ventral horn motor neurons of cervical (a and b) and thoracic (c and d) spinal cord segments from dog Y. Bar in (c) indicates magnification for all 4 micrographs

the neurobehavioral deficits in the affected dogs. Similar brain atrophy has been reported in human subjects with CLN5 disease (Holmberg et al., 2000; Santavuori et al., 2001). Thus, any therapeutic interventions that inhibit the progression of this atrophy in the dog model are likely to be effective in treating the human disease. The brain atrophy characteristic of CLN5 disease in both dogs and humans appears to be global and is not restricted to specific brain regions or neuron types. Therefore, to be most effective, any therapeutic intervention would need to target the entire central nervous system.

The original identification of the canine CLN5 disorder in Golden Retrievers was performed by evaluating privately owned dogs (Gilliam et al., 2015). In a home environment, it was possible to maintain the affected dogs up to as much as 34 months of age. At ages beyond the 23.4 months over which the dogs in this study were followed, affected dogs developed more severe aggressive behavior, seizures, visual impairment and cognitive decline. In a research setting, it would be logistically and ethically difficult to allow the disease to progress to the later stages, particularly due to the risks of injuries to the dogs and their handlers. To assess the benefits of therapeutic interventions using the dog model, it would likely be suffi-

cient to evaluate the efficacy of these interventions in inhibiting the development and progression of signs that become apparent by 2 years of age. However, if the design of a therapeutic intervention study required following a control group of dogs to late-stage clinical disease, for example to assess the efficacy of therapeutic interventions initiated late in the disease progression, it would be beneficial to breed the disease variant into a smaller dog breed in which the advanced disease signs could be more effectively managed in a research setting.

CLN5 disease, like most other NCLs, is an autosomal recessively inherited disorder affecting both males and females with equal frequencies. No sex differences in disease phenotypes have been reported for human patients. Likewise, there was no significant difference in clinical disease progression and tissue pathology between the male and female littermates evaluated in this study.

In previous studies, it has been demonstrated that other forms of NCL are associated with low plasma concentrations of carnitine (Katz, 1996; Katz & Siakotos, 1995), and that in animal models dietary carnitine supplementation can slow disease progression (Katz et al., 1997; Siakotos et al., 2001).

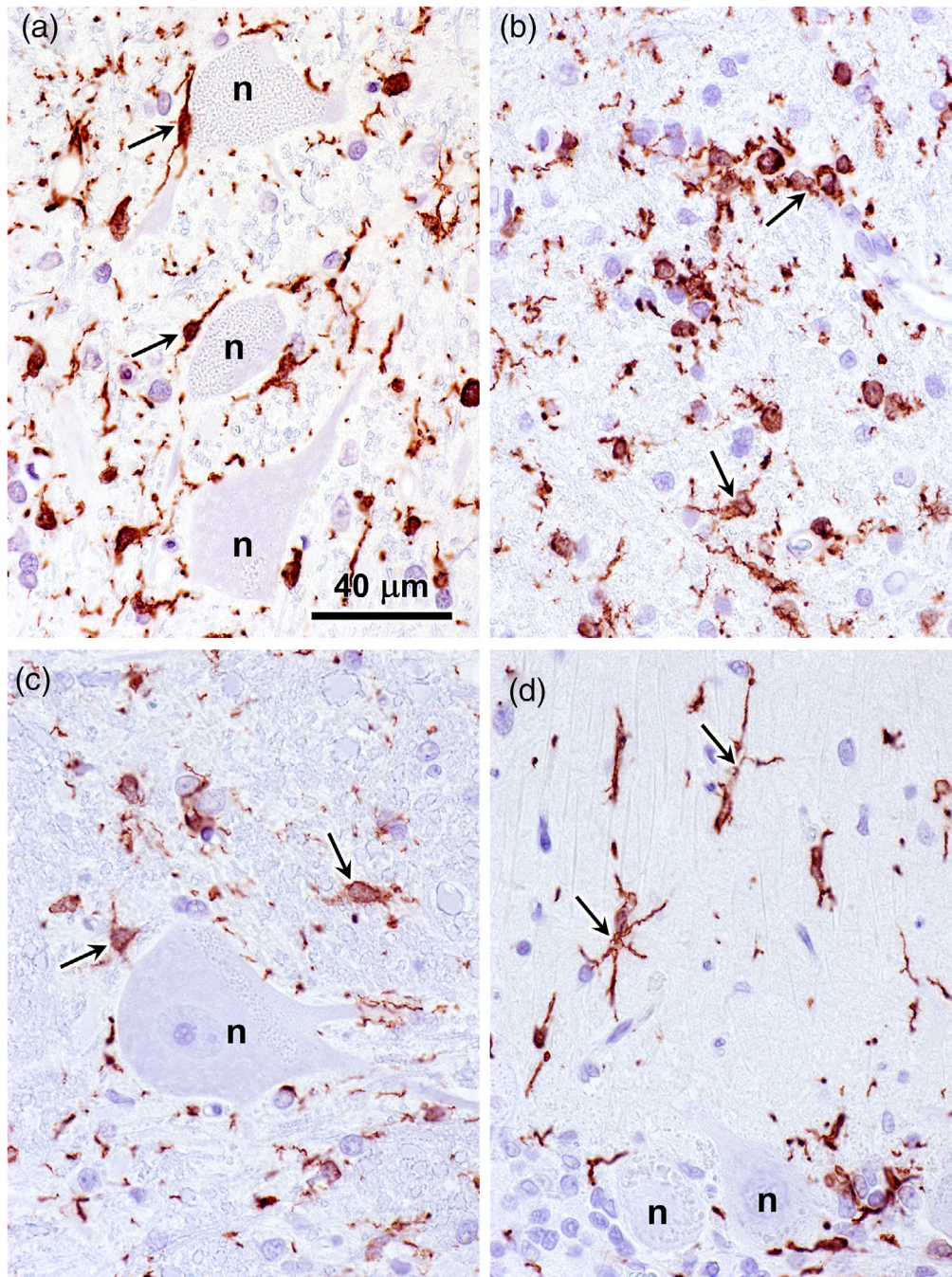


FIGURE 9 Light micrographs of sections of thoracic spinal cord ventral horn (a), occipital cortex (b), deep cerebellar nucleus (c), and cerebellar cortex (d) from dog Z. Sections were immunostained for Iba1, a marker for activated microglia. Representative immunostained cells are indicated by arrows. Large neurons indicated by n. Bar in (a) indicates magnification for all four micrographs

The primary role of carnitine is facilitation of mitochondrial fatty acid metabolism. Fatty acids are transported into mitochondria as carnitine esters where they are then metabolized through beta oxidation for energy production (Adeva-Andany et al., 2019; Bremer, 1983; Houten et al., 2020; Schlaepfer & Joshi, 2020). In most mammals, including humans and dogs, tissue carnitine levels are determined by a combination of dietary intake and endogenous biosynthesis (Bach, 1982; Duran et al., 1990; Giovannini et al., 1991). Carnitine

is biosynthesized from 6-N-trimethyllysine (TML) that is in turn generated by the degradation of proteins in which specific lysine residues have been enzymatically trimethylated (Maas et al., 2020). In various forms of NCL, including CLN5 disease, a major component of the lysosomal storage material is the subunit c protein of the mitochondrial membrane ATP synthase complex (Frugier et al., 2008; Ranta et al., 2001; Tyynelä et al., 1997). The subunit c protein contains two lysine residues, one of which is trimethylated, both in mitochondria

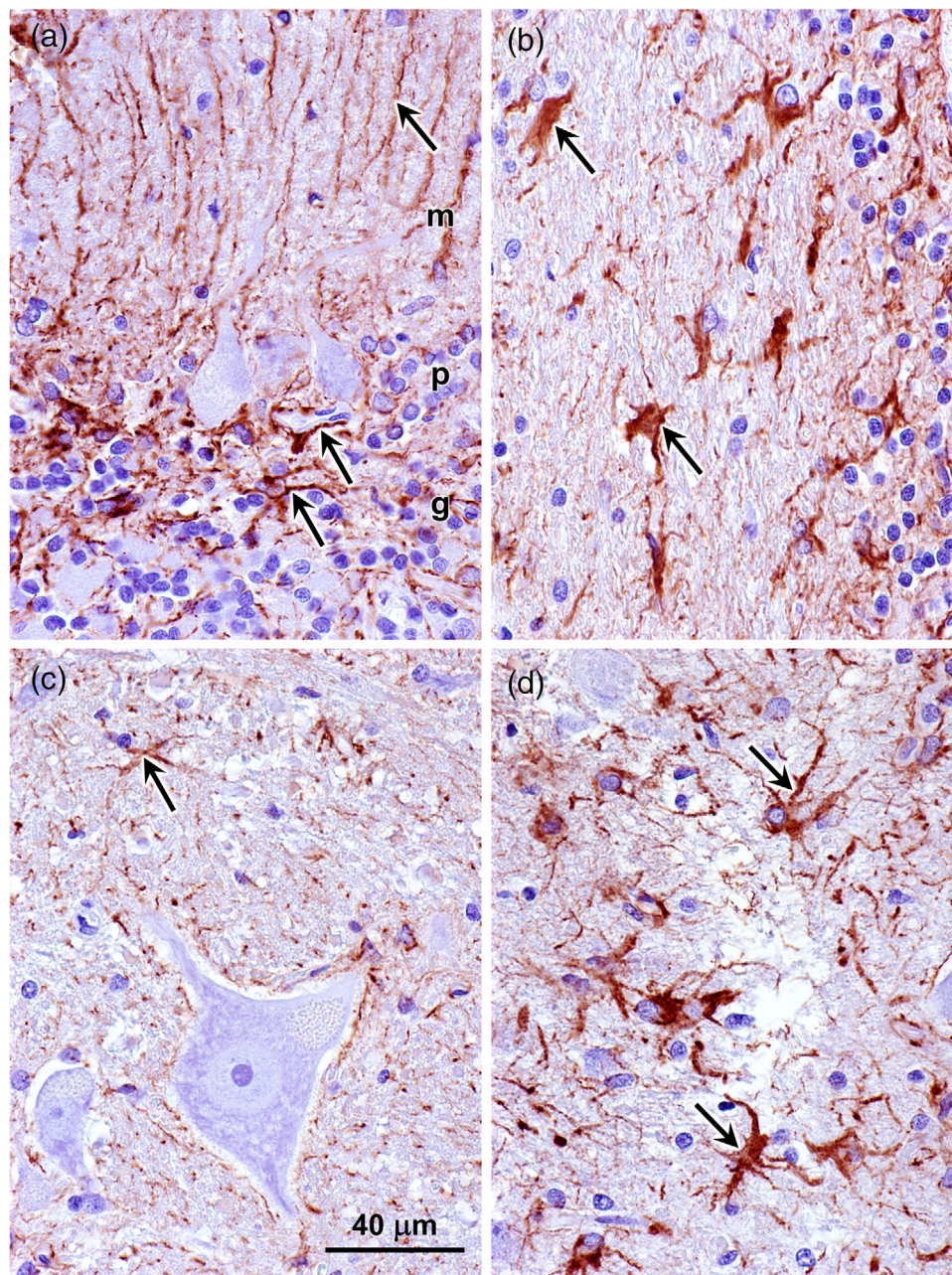


FIGURE 10 Light micrographs of sections of cerebellar cortex (a and b), deep cerebellar nucleus (c), and occipital cortex (d) from dog Z. Sections were immunostained for GFAP, a maker for activated astrocytes. Representative immunostained cells are indicated by arrows. Layers of the cerebellar cortex in (a) are molecular layer (m), Purkinje cell layer (p), and granule cell layer (g). Area shown in (b) is the white matter layer just interior to the granule cell layer. Bar in (c) indicates magnification for all four micrographs

and in the NCL-specific storage bodies (Chen et al., 2004; Katz et al., 1994, 1995). In previous studies, it was found that plasma carnitine concentrations are low in the CLN8 form of canine NCL and in human subjects with the CLN3 form of NCL (Katz, 1996; Katz & Siakotos, 1995). Patients with CLN3 disease had significantly lower plasma TML concentrations than their healthy relatives (Katz, 1996). These findings suggested that TML derived from the normal turnover of the subunit c protein is a major precursor for carnitine biosynthesis. The finding that dogs with CLN5 disease also have low

plasma carnitine levels is consistent with this hypothesis. It is not known whether the low carnitine levels contribute to the CLN5 disease pathogenesis, but dietary supplementation with carnitine did slow disease progression in mice and dogs with the CLN8 form of NCL (Katz et al., 1997; Siakotos et al., 2001). The data from the Golden Retriever CLN5 disease suggest that studies should be undertaken to determine whether blood levels of carnitine are low in children with this disorder, and if so, whether carnitine supplementation can have a therapeutic benefit.

Although the NCLs are primarily recognized as neurological disorders, it has been established that cardiac pathology also occurs in multiple forms of NCL in both human subjects and in animal models, including dogs (Rietdorf et al., 2020). However, to our knowledge, this is the first report of cardiac pathology in CLN5 disease. As with other canine NCLs (Katz, Rustad, et al., 2017), dogs with the CLN5 disorder exhibited accumulation of lysosomal storage bodies in cardiac muscle. Whether this was accompanied by cardiac dysfunction was not determined. Cardiac pathology is often characterized by elevations in blood levels of cardiac troponin. Among the affected Golden Retrievers, one exhibited a modest elevation in plasma troponin at about 23 months of age. The dogs had to be euthanized before reaching end-stage neurological disease, so it was not possible to determine whether this was an early indication of overt cardiac pathology late in the disease process that would have progressed over time. In dogs with the CLN2 form of NCL, it was found that if lifespan was extended with central nervous system gene therapy, there was a pronounced progressive elevation in plasma cardiac troponin concentrations and development of cardiac dysfunction (Katz, Johnson, et al., 2017). The data from the current study suggest that similar cardiac pathology may become apparent in the CLN5 disorder late in the disease progression. Determining whether this is the case will be important in developing strategies for therapeutic interventions for this disease.

The ultrastructural appearances of the neuronal storage body contents in the affected Golden Retrievers were similar to those reported for neuronal tissue from human CLN5 disease patients (Tyynelä et al., 1997), and from other dogs, sheep and mice with CLN5 disease (Frugier et al., 2008; Gilliam et al., 2015; Kolicheski et al., 2016; Kopra et al., 2004; Villani et al., 2019). The fact that the subunit c protein of inner mitochondrial membrane ATP synthase complex is a major component of the storage bodies suggests that the membrane-like components of these cellular inclusions may be derived from mitochondrial membranes that enter the storage body-forming pathway via autophagy. Apparently, insufficiency of CLN5 results in a specific impairment of subunit c degradation, perhaps related to the hydrophobic nature of the subunit c protein.

Neuroinflammation, reflected by activation of neural tissue astrocytes and microglia, is a common feature of the NCLs as well as other progressive neurodegenerative disorders (Cervellati et al., 2020; Palmer et al., 2013; Shyng & Sands, 2014). Astrocyte and microglial activation were observed in the brain and spinal cord of the CLN5-affected dogs, indicating that these animals recapitulate this component of the human disease process. There is evidence that activated astrocytes and microglia contribute to neural tissue pathogenesis (Groh et al., 2016, 2017; Kohlschütter et al., 2019; Macauley et al., 2014). It should be possible to assess whether this is the case in the canine CLN5 disease model

by investigating whether pharmacological interventions that inhibit glial activation have therapeutic benefits.

In conclusion, the canine disease associated with the *CLN5* c.934_935delAG variant is likely to serve as a good model for developing a better understanding of the mechanisms underlying human CLN5 disease and for assessing the efficacy of potential treatments for this disorder. The canine disorder recapitulates the human disease phenotype very well. Data from the dog model suggest potential novel approaches to therapy. The discovery that dogs with this disorder have low blood carnitine levels suggest that dietary carnitine supplementation could have a therapeutic benefit, either alone or in conjunction with another mode of therapeutic intervention. The presence of widespread neuroinflammation suggests that anti-inflammatory treatments directed to the central nervous system may also ameliorate disease progression. Future studies that employ the canine model are likely to advance the endeavor to develop an effective treatment for CLN5 disease. A sheep model for CLN5 disease has already proven useful in gene therapy studies (Mitchell et al., 2018; Murray et al., 2021). The sheep and canine disorders are similar in many aspects (Frugier et al., 2008; Mitchell et al., 2018; Murray et al., 2021). For example, both are characterized by progressive neurological signs, brain atrophy, and intracellular accumulation of autofluorescent storage bodies in brain neurons. Both the sheep and dog disorders appear to be good models for the human disease. However, the dog model may be more practical to use in most research settings.

ACKNOWLEDGMENTS

Our thanks to Jon Gangotti of the University of California San Diego Biochemical Genetics & Metabolomics Laboratory for performing the plasma carnitine analyses. This research was supported by U.S. National Institutes of Health grant EY031674, a BioNexus KC grant, and a University of Missouri Life Sciences graduate fellowship (GRK).

CONFLICT OF INTEREST

The authors have no conflicts of interest to report.

AUTHOR CONTRIBUTIONS

All authors had full access to all the data in the study and take responsibility for the integrity of the data and the accuracy of the data analysis. *Conceptualization*: Martin L. Katz. *Methodology*, Elizabeth J. Meiman, Grace Robinson Kick, Cheryl A. Jensen, Joan R. Coates, and Martin L. Katz. *Investigation*: Elizabeth J. Meiman, Grace Robinson Kick, Cheryl A. Jensen, and Martin L. Katz. *Formal Analysis*: Elizabeth J. Meiman, Grace Robinson Kick, Joan R. Coates, and Martin L. Katz. *Resources*: Martin L. Katz; *Writing—original draft*: Elizabeth J. Meiman, Grace Robinson Kick, and Martin L. Katz. *Writing—review & editing*: Elizabeth J. Meiman, Grace Robinson Kick, Cheryl A. Jensen, Joan R. Coates, and Martin

L. Katz. *Visualization*: Elizabeth J. Meiman, Grace Robinson Kick, and Martin L. Katz. *Supervision*: Joan R. Coates, and Martin L. Katz. *Funding acquisition*: Martin L. Katz.

DATA AVAILABILITY STATEMENT

The data that support the findings of this study are available within the article and its supporting information files.

ORCID

Elizabeth J. Meiman  <https://orcid.org/0000-0002-0231-3591>

Martin L. Katz  <https://orcid.org/0000-0002-2582-9187>

REFERENCES

- Adeva-Andany, M. M., Carneiro-Freire, N., Seco-Filgueira, M., Fernández-Fernández, C., & Mouriño-Bayolo, D. (2019). Mitochondrial β -oxidation of saturated fatty acids in humans. *Mitochondrion*, *46*, 73–90. <https://doi.org/10.1016/j.mito.2018.02.009>
- Autti, T., Raininko, R., Launes, J., Nuutila, A., & Santavuori, P. (1992). Jansky-Bielschowsky variant disease: CT, MRI, and SPECT findings. *Pediatric Neurology*, *8*, 121–126. [https://doi.org/10.1016/0887-8994\(92\)90032-T](https://doi.org/10.1016/0887-8994(92)90032-T)
- Bach, A. C. (1982). Carnitine in human nutrition. *Zeitschrift für Ernährungswissenschaft*, *21*, 257–265. <https://doi.org/10.1007/BF02020743>
- Basak, I., Wicky, H. E., McDonald, K. O., Xu, J. B., Palmer, J. E., Best, H. L., Lefrancois, S., Lee, S. Y., Schoderboeck, L., & Hughes, S. M. (2021). A lysosomal enigma CLN5 and its significance in understanding neuronal ceroid lipofuscinosis. *Cellular and Molecular Life Sciences*, *78*, 4735–4763. <https://doi.org/10.1007/s00018-021-03813-x>
- Beck-Wödl, S., Harzer, K., Sturm, M., Buchert, R., Rieß, O., Mennel, H. D., Latta, E., Pagenstecher, A., & Keber, U. (2018). Homozygous TBC1 domain-containing kinase (TBCK) mutation causes a novel lysosomal storage disease—A new type of neuronal ceroid lipofuscinosis (CLN15)? *Acta Neuropathologica Communications*, *6*, 145. <https://doi.org/10.1186/s40478-018-0646-6>
- Bible, E., Gupta, P., Hofmann, S. L., & Cooper, J. D. (2004). Regional and cellular neuropathology in the palmitoyl protein thioesterase-1 null mutant mouse model of infantile neuronal ceroid lipofuscinosis. *Neurobiology of Disease*, *16*, 346–359. <https://doi.org/10.1016/j.nbd.2004.02.010>
- Bockenbauer, D., & Kleta, R. (2017). Of dogs and men. *European Journal of Human Genetics*, *25*, 161. <https://doi.org/10.1038/ejhg.2016.161>
- Bremer, J. (1983). Carnitine—metabolism and functions. *Physiological Reviews*, *63*, 1420–1480. <https://doi.org/10.1152/physrev.1983.63.4.1420>
- Butz, E. S., Chandrachud, U., Mole, S. E., & Cotman, S. L. (2020). Moving towards a new era of genomics in the neuronal ceroid lipofuscinoses. *Biochimica et Biophysica Acta - Molecular Basis of Disease*, *1866*, 165571. <https://doi.org/10.1016/j.bbadis.2019.165571>
- Carroll, J. A., & Chesebro, B. (2019). Neuroinflammation, microglia, and cell-association during prion disease. *Viruses*, *11*, 65. <https://doi.org/10.3390/v11010065>
- Cervellati, C., Trentini, A., Pecorelli, A., & Valacchi, G. (2020). Inflammation in neurological disorders: The thin boundary between brain and periphery. *Antioxidants & Redox Signaling*, *33*, 191–210. <https://doi.org/10.1089/ars.2020.8076>
- Chen, R., Fearnley, I. M., Palmer, D. N., & Walker, J. E. (2004). Lysine 43 is trimethylated in subunit c from bovine mitochondrial ATP synthase and in storage bodies associated with Batten Disease*. *Journal of Biological Chemistry*, *279*, 21883–21887. <https://doi.org/10.1074/jbc.M402074200>
- De Silva, B., Adams, J., & Lee, S. Y. (2015). Proteolytic processing of the neuronal ceroid lipofuscinosis related lysosomal protein CLN5. *Experimental Cell Research*, *338*, 45–53. <https://doi.org/10.1016/j.yexcr.2015.08.021>
- Duran, M., Loof, N. E., Ketting, D., & Dorland, L. (1990). Secondary carnitine deficiency. *Journal of Clinical Chemistry and Clinical Biochemistry. Zeitschrift für klinische Chemie und klinische Biochemie*, *28*, 359–363.
- Fletcher, J. L., & Taylor, R. M. (2016). Therapy development for the lysosomal storage disease fucosidosis using the canine animal model. *Pediatric endocrinology reviews*, *13*, 697–706.
- Frugier, T., Mitchell, N. L., Tammen, I., Houweling, P. J., Arthur, D. G., Kay, G. W., vanDiggelen, O. P., Jolly, R. D., & Palmer, D. N. (2008). A new large animal model of CLN5 neuronal ceroid lipofuscinosis in Borderdale sheep is caused by a nucleotide substitution at a consensus splice site (c.571+1G>A) leading to excision of exon 3. *Neurobiology of Disease*, *29*, 306–315. <https://doi.org/10.1016/j.nbd.2007.09.006>
- Gelatt, K.N., Gilger, B.C., & Kern, T.J. (Eds.). (2013) *Veterinary ophthalmology* (5th ed.). John Wiley & Sons, Inc.
- Gilliam, D., Kolichski, A., Johnson, G. S., Mhlanga-Mutangadura, T., Taylor, J. F., Schnabel, R. D., & Katz, M. L. (2015). Golden Retriever dogs with neuronal ceroid lipofuscinosis have a two-base-pair deletion and frameshift in CLN5. *Molecular Genetics and Metabolism*, *115*, 101–109. <https://doi.org/10.1016/j.ymgme.2015.04.001>
- Giovannini, M., Agostoni, C., & Salari, P. C. (1991). Is carnitine essential in children? *Journal of International Medical Research*, *19*, 88–102. <https://doi.org/10.1177/030006059101900202>
- Groh, J., Berve, K., & Martini, R. (2017). Fingolimod and teriflunomide attenuate neurodegeneration in mouse models of neuronal ceroid lipofuscinosis. *Molecular Therapy*, *25*, 1889–1899. <https://doi.org/10.1016/j.yjth.2017.04.021>
- Groh, J., Kühl, T. G., Ip, C. W., Nelvagal, H. R., Sri, S., Duckett, S., Mirza, M., Langmann, T., Cooper, J. D., & Martini, R. (2013). Immune cells perturb axons and impair neuronal survival in a mouse model of infantile neuronal ceroid lipofuscinosis. *Brain*, *136*, 1083–1101. <https://doi.org/10.1093/brain/awt020>
- Groh, J., Ribechini, E., Stadler, D., Schilling, T., Lutz, M. B., & Martini, R. (2016). Sialoadhesin promotes neuroinflammation-related disease progression in two mouse models of CLN disease. *Glia*, *64*, 792–809. <https://doi.org/10.1002/glia.22962>
- Haltia, M., Herva, R., Suopanki, J., Baumann, M., & Tyynelä, J. (2001). Hippocampal lesions in the neuronal ceroid lipofuscinoses. *European Journal of Paediatric Neurology*, *5*, 209–211. <https://doi.org/10.1053/eipn.2000.0464>
- Hampel, H., Caraci, F., Cuello, A. C., Caruso, G., Nisticò, R., Corbo, M., Baldacci, F., Toschi, N., Garaci, F., Chiesa, P. A., Verdooner, S. R., Akman-Anderson, L., Hernández, F., Ávila, J., Emanuele, E., Valenzuela, P. L., Lucía, A., Watling, M., Imbimbo, B. P., ... Lista, S. (2020). A path toward precision medicine for neuroinflammatory mechanisms in Alzheimer's Disease. *Frontiers in Immunology*, *11*, 456. <https://doi.org/10.3389/fimmu.2020.00456>

- Holmberg, V., Lauronen, L., Autti, T., Santavuori, P., Savukoski, M., Uvebrant, P., Hofman, I., Peltonen, L., & Järvelä, I. (2000). Phenotype-genotype correlation in eight patients with Finnish variant late infantile NCL (CLN5). *Neurology*, *55*, 579–581. <https://doi.org/10.1212/WNL.55.4.579>
- Houten, S. M., Wanders, R. J. A., & Ranea-Robles, P. (2020). Metabolic interactions between peroxisomes and mitochondria with a special focus on acylcarnitine metabolism. *Biochimica et Biophysica Acta (BBA)—Molecular Basis of Disease*, *1866*, 165720. <https://doi.org/10.1016/j.bbadis.2020.165720>
- Houweling, P. J., Cavanagh, J. A. L., Palmer, D. N., Frugier, T., Mitchell, N. L., Windsor, P. A., Raadsma, H. W., & Tammen, I. (2006). Neuronal ceroid lipofuscinosis in Devon cattle is caused by a single base duplication (c.662dupG) in the bovine CLN5 gene. *Biochimica et Biophysica Acta - Molecular Basis of Disease*, *1762*, 890–897. <https://doi.org/10.1016/j.bbadis.2006.07.008>
- Jules, F., Sauvageau, E., Dumaresq-Doiron, K., Mazzaferri, J., Haug-Kröper, M., Fluhrer, R., Costantino, S., & Lefrançois, S. (2017). CLN5 is cleaved by members of the SPP/SPPL family to produce a mature soluble protein. *Experimental Cell Research*, *357*, 40–50. <https://doi.org/10.1016/j.yexcr.2017.04.024>
- Katz, M. L. (1996). Decreased plasma carnitine and trimethyl-L-lysine levels associated with lysosomal accumulation of a trimethyl-L-lysine containing protein in Batten disease. *Biochimica et Biophysica Acta—Molecular Basis of Disease*, *1317*, 192–198. [https://doi.org/10.1016/S0925-4439\(96\)00054-3](https://doi.org/10.1016/S0925-4439(96)00054-3)
- Katz, M. L., Buckley, R. M., Biegen, V., O'Brien, D. P., Johnson, G. C., Warren, W. C., & Lyons, L. A. (2020). Neuronal Ceroid Lipofuscinosis in a domestic cat associated with a DNA sequence variant that creates a premature stop codon in CLN6. *Genes|Genomes|Genetics*, *10*, 2741. <https://doi.org/10.1534/g3.120.401407>
- Katz, M. L., Christianson, J. S., Norbury, N. E., Gao, C., Siakotos, A. N., & Koppang, N. (1994). Lysine methylation of mitochondrial ATP synthase subunit c stored in tissues of dogs with hereditary ceroid lipofuscinosis. *Journal of Biological Chemistry*, *269*, 9906–9911.
- Katz, M. L., Coates, J. R., Sibigtroth, C. M., Taylor, J. D., Carpentier, M., Young, W. M., Winger, F. A., Kennedy, D., Vuilleminot, B. R., & O'Neill, C. A. (2014). Enzyme replacement therapy attenuates disease progression in a canine model of late-infantile neuronal ceroid lipofuscinosis (CLN2 Disease). *Journal of Neuroscience Research*, *92*, 1591–1598. <https://doi.org/10.1002/jnr.23423>
- Katz, M. L., Gao, C. L., Tompkins, J. A., Bronson, R. T., & Chin, D. T. (1995). Mitochondrial ATP synthase subunit c stored in hereditary ceroid-lipofuscinosis contains trimethyl-lysine. *Biochemical Journal*, *310*, 887–892. <https://doi.org/10.1042/bj3100887>
- Katz, M. L., Johnson, G. C., Leach, S. B., Williamson, B. G., Coates, J. R., Whiting, R. E. H., Vansteenkiste, D. P., & Whitney, M. S. (2017). Extraneuronal pathology in a canine model of CLN2 neuronal ceroid lipofuscinosis after intracerebroventricular gene therapy that delays neurological disease progression. *Gene Therapy*, *24*, 215–223. <https://doi.org/10.1038/gt.2017.4>
- Katz, M. L., & Redmond, M. T. (2001). Effect of Rpe65 knockout on accumulation of lipofuscin fluorophores in the retinal pigment epithelium. *Investigative Ophthalmology and Visual Science*, *42*, 3023–3030.
- Katz, M. L., Rice, L. M., & Gao, C.-L. (1997). Dietary carnitine supplements slow disease progression in a putative mouse model for hereditary ceroid-lipofuscinosis. *Journal of Neuroscience Research*, *50*, 123–132. [https://doi.org/10.1002/\(SICI\)1097-4547\(19971001\)50:1<123::AID-JNR13>3.0.CO;2-C](https://doi.org/10.1002/(SICI)1097-4547(19971001)50:1<123::AID-JNR13>3.0.CO;2-C)
- Katz, M. L., Rustad, E., Robinson, G. O., Whiting, R. E. H., Student, J. T., Coates, J. R., & Narfstrom, K. (2017). Canine neuronal ceroid lipofuscinoses: Promising models for preclinical testing of therapeutic interventions. *Neurobiology of Disease*, *108*, 277–287. <https://doi.org/10.1016/j.nbd.2017.08.017>
- Katz, M. L., & Siakotos, A. N. (1995). Canine hereditary ceroid-lipofuscinosis: Evidence for a defect in the carnitine biosynthetic pathway. *American Journal of Medical Genetics*, *57*, 266–271. <https://doi.org/10.1002/ajmg.1320570231>
- Katz, M. L., Tecedor, L., Chen, Y., Williamson, B. G., Lysenko, E., Winger, F. A., Young, W. M., Johnson, G. C., Whiting, R. E. H., Coates, J. R., & Davidson, B. L. (2015). AAV gene transfer delays disease onset in a TPP1-deficient canine model of the late infantile form of Batten disease. *Science Translational Medicine*, *7*, 313ra180–313ra180. <https://doi.org/10.1126/scitranslmed.aac6191>
- Katz, M. L., Wendt, K. D., & Sanders, D. N. (2005). RPE65 gene mutation prevents development of autofluorescence in retinal pigment epithelial phagosomes. *Mechanisms of Ageing and Development*, *126*, 513–521. <https://doi.org/10.1016/j.mad.2004.11.004>
- Kaur, D., Sharma, V., & Deshmukh, R. (2019). Activation of microglia and astrocytes: A roadway to neuroinflammation and Alzheimer's disease. *Inflammopharmacology*, *27*, 663–677. <https://doi.org/10.1007/s10787-019-00580-x>
- Kay, G. W., & Palmer, D. N. (2013). Chronic oral administration of minocycline to sheep with ovine CLN6 neuronal ceroid lipofuscinosis maintains pharmacological concentrations in the brain but does not suppress neuroinflammation or disease progression. *Journal of Neuroinflammation*, *10*, 900. <https://doi.org/10.1186/1742-2094-10-97>
- Kick, G. R., Meiman, E. J., Sabol, J. C., Whiting, R. E. H., Ota-Kuroki, J., Castaner, L. J., Jensen, C. A., & Katz, M. L. (2021). Visual system pathology in a canine model of CLN5 neuronal ceroid lipofuscinosis. *Experimental Eye Research*, *210*, 108686. <https://doi.org/10.1016/j.exer.2021.108686>
- King, B., Marshall, N. R., Hassiotis, S., Trim, P. J., Tucker, J., Hattersley, K., Snel, M. F., Jolly, R. D., Hopwood, J. J., & Hemsley, K. M. (2017). Slow, continuous enzyme replacement via spinal CSF in dogs with the paediatric-onset neurodegenerative disease. *MPS IIIA. Journal of Inherited Metabolic Disease*, *40*, 443–453. <https://doi.org/10.1007/s10545-016-9994-1>
- Kirveskari, E., Partinen, M., & Santavuori, P. (2001). Sleep and its disturbance in a variant form of late infantile neuronal ceroid lipofuscinosis (CLNS). *Journal of Child Neurology*, *16*, 707–713. <https://doi.org/10.1177/088307380101601001>
- Kohlschütter, A., Schulz, A., Bartsch, U., & Storch, S. (2019). Current and emerging treatment strategies for neuronal ceroid lipofuscinoses. *CNS Drugs*, *33*, 315–325. <https://doi.org/10.1007/s40263-019-00620-8>
- Kolichski, A., Johnson, G. S., O'Brien, D. P., Mhlanga-Mutangadura, T., Gilliam, D., Guo, J., Anderson-Sieg, T. D., Schnabel, R. D., Taylor, J. F., Lebowitz, A., Swanson, B., Hicks, D., Niman, Z. E., Winger, F. A., Carpentier, M. C., & Katz, M. L. (2016). Australian cattle dogs with neuronal ceroid lipofuscinosis are homozygous for a CLN5 nonsense mutation previously identified in Border Collies. *Journal of Veterinary Internal Medicine*, *30*, 1149–1158. <https://doi.org/10.1111/jvim.13971>

- Kondagari, G. S., Fletcher, J. L., Cruz, R., Williamson, P., Hopwood, J. J., & Taylor, R. M. (2015). The effects of intracisternal enzyme replacement versus sham treatment on central neuropathology in pre-clinical canine fucosidosis. *Orphanet Journal of Rare Diseases*, *10*, 1–12. <https://doi.org/10.1186/s13023-015-0357-z>
- Kopra, O., Vesa, J., vonSchantz, C., Manninen, T., Minye, H., Fabritius, A. L., Rapola, J., vanDiggelen, O. P., Saarela, J., Jalanko, A., & Peltonen, L. (2004). A mouse model for Finnish variant late infantile neuronal ceroid lipofuscinosis, CLN5, reveals neuropathology associated with early aging. *Human Molecular Genetics*, *13*, 2893–2906. <https://doi.org/10.1093/hmg/ddh312>
- Kovacs, G. G. (2018). Cellular reactions of the central nervous system. *Handbook of clinical neurology* (1st ed., pp. 13–23). Elsevier. <https://doi.org/10.1016/B978-0-12-802395-2.00003-1>
- Larkin, H., Ribeiro, M. G., & Lavoie, C. (2013). Topology and membrane anchoring of the lysosomal storage disease-related protein CLN5. *Human Mutation*, *34*, 1688–1697. <https://doi.org/10.1002/humu.22443>
- Lebrun, A.-H., Storch, S., Rüschemdorf, F., Schmiedt, M.-L., Kyttälä, A., Mole, S. E., Kitzmüller, C., Saar, K., Mewasingh, L. D., Boda, V., Kohlschütter, A., Ullrich, K., Braulke, T., & Schulz, A. (2009). Retention of lysosomal protein CLN5 in the endoplasmic reticulum causes neuronal ceroid lipofuscinosis in Asian Sibship. *Human Mutation*, *30*, E651–E661. <https://doi.org/10.1002/humu.21010>
- Leinonen, H., Keksa-Goldsteine, V., Ragauskas, S., Kohlmann, P., Singh, Y., Savchenko, E., Puranen, J., Malm, T., Kalesnykas, G., Koistinaho, J., Tanila, H., & Kanninen, K. M. (2017). Retinal degeneration in a mouse model of CLN5 Disease Is associated with compromised autophagy. *Scientific Reports*, *7*, 1–12. <https://doi.org/10.1038/s41598-017-01716-1>
- Lewis, G., Morrill, A. M., Conway-Allen, S. L., & Kim, B. (2019). Review of Cerliponase Alfa: Recombinant human enzyme replacement therapy for Late-Infantile Neuronal Ceroid Lipofuscinosis Type 2. *Journal of Child Neurology*, *35*, 348–353. <https://doi.org/10.1177/0883073819895694>
- Liberman, A. C., Trias, E., Da Silva Chagas, L., Trindade, P., Dos Santos Pereira, M., Refojo, D., Hedin-Pereira, C., & Serfaty, C. A. (2019). Neuroimmune and inflammatory signals in complex disorders of the central nervous system. *Neuroimmunomodulation*, *25*, 246–270. <https://doi.org/10.1159/000494761>
- Linnerbauer, M., & Rothhammer, V. (2020). Protective functions of reactive astrocytes following central nervous system insult. *Frontiers in Immunology*, *11*, 1–18. <https://doi.org/10.3389/fimmu.2020.573256>
- Linnerbauer, M., Wheeler, M. A., & Quintana, F. J. (2020). Astrocyte crosstalk in CNS inflammation. *Neuron*, *108*, 608–622. <https://doi.org/10.1016/j.neuron.2020.08.012>
- Löbel, U., Sedlacik, J., Nickel, M., Lezius, S., Fiehler, J., Nestrail, I., Kohlschütter, A., & Schulz, A. (2016). Volumetric description of brain atrophy in neuronal ceroid lipofuscinosis 2: Supratentorial gray matter shows uniform disease progression. *American Journal of Neuroradiology*, *37*, 1938–1943. <https://doi.org/10.3174/ajnr.A4816>
- Lorenz, M. D., Coates, J. R., & Kent, M. (2011). Neurologic history, neuroanatomy, and neurologic examination. *Handbook of Veterinary Neurology*, 2–36. <https://doi.org/10.1016/b978-1-4377-0651-2.10001-3>
- Lynch, M. A. (2020). Can the emerging field of immunometabolism provide insights into neuroinflammation? *Progress in Neurobiology*, *184*, 101719. <https://doi.org/10.1016/j.pneurobio.2019.101719>
- Maas, M. N., Hintzen, J. C. J., Porzberg, M. R. B., & Mecinović, J. (2020). Trimethyllysine: From carnitine biosynthesis to epigenetics. *International Journal of Molecular Sciences*, *21*, 9451. <https://doi.org/10.3390/ijms21249451>
- Macauley, S. L., Wong, A. M. S., Shyng, C., Augner, D. P., Dearborn, J. T., Pearse, Y., Roberts, M. S., Fowler, S. C., Cooper, J. D., Watterson, D. M., & Sands, M. S. (2014). An anti-neuroinflammatory that targets dysregulated glia enhances the efficacy of CNS-directed gene therapy in murine Infantile Neuronal Ceroid Lipofuscinosis. *Journal of Neuroscience*, *34*, 13077–13082. <https://doi.org/10.1523/JNEUROSCI.2518-14.2014>
- Macauley, S. L., Wozniak, D. F., Kielar, C., Tan, Y., Cooper, J. D., & Sands, M. S. (2009). Cerebellar pathology and motor deficits in the palmitoyl protein thioesterase 1-deficient mouse. *Experimental Neurology*, *217*, 124–135. <https://doi.org/10.1016/j.expneurol.2009.01.022>
- Mamo, A., Jules, F., Dumaresq-Doiron, K., Costantino, S., & Lefrançois, S. (2012). The role of ceroid lipofuscinosis neuronal protein 5 (CLN5) in endosomal sorting. *Molecular and Cellular Biology*, *32*, 1855–1866. <https://doi.org/10.1128/mcb.06726-11>
- Melville, S. A., Wilson, C. L., Chiang, C. S., Studdert, V. P., Lingaas, F., & Wilton, A. N. (2005). A mutation in canine CLN5 causes neuronal ceroid lipofuscinosis in Border collie dogs. *Genomics*, *86*, 287–294. <https://doi.org/10.1016/j.ygeno.2005.06.005>
- Mendsaikhan, A., Tooyama, I., & Walker, D. G. (2019). Microglial progulin: Involvement in Alzheimer's Disease and neurodegenerative diseases. *Cells*, *8*, 230. <https://doi.org/10.3390/cells8030230>
- Mitchell, N. L., Russell, K. N., Wellby, M. P., Wicky, H. E., Schoderboeck, L., Barrell, G. K., Melzer, T. R., Gray, S. J., Hughes, S. M., & Palmer, D. N. (2018). Longitudinal in vivo monitoring of the CNS demonstrates the efficacy of gene therapy in a sheep model of CLN5 Batten Disease. *Molecular Therapy*, *26*, 2366–2378. <https://doi.org/10.1016/j.ymthe.2018.07.015>
- Moharir, A., Peck, S. H., Budden, T., & Lee, S. Y. (2013). The role of N-Glycosylation in folding, trafficking, and functionality of lysosomal protein CLN5. *PLoS One*, *8*, e74299. <https://doi.org/10.1371/journal.pone.0074299>
- Morgan, B. R., Coates, J. R., Johnson, G. C., Bujnak, A. C., & Katz, M. L. (2013). Characterization of intercostal muscle pathology in canine degenerative myelopathy: A disease model for amyotrophic lateral sclerosis. *Journal of Neuroscience Research*, *91*, 1639–1650. <https://doi.org/10.1002/jnr.23287>
- Murray, S. J., Russell, K. N., Melzer, T. R., Gray, S. J., Heap, S. J., Palmer, D. N., & Mitchell, N. L. (2021). Intravitreal gene therapy protects against retinal dysfunction and degeneration in sheep with CLN5 Batten disease. *Experimental Eye Research*, *207*, 108600. <https://doi.org/10.1016/j.exer.2021.108600>
- Oswald, M. J., Palmer, D. N., Kay, G. W., Shemilt, S. J. A., Rezaie, P., & Cooper, J. D. (2005). Glial activation spreads from specific cerebral foci and precedes neurodegeneration in presymptomatic ovine neuronal ceroid lipofuscinosis (CLN6). *Neurobiology of Disease*, *20*, 49–63. <https://doi.org/10.1016/j.nbd.2005.01.025>
- Palmer, D. N., Barry, L. A., Tyynelä, J., & Cooper, J. D. (2013). NCL disease mechanisms. *Biochimica et Biophysica Acta—Molecular Basis of Disease*, *1832*, 1882–1893. <https://doi.org/10.1016/j.bbdis.2013.05.014>
- Partridge, B., & Rossmeisl, J. H. (2020). Companion animal models of neurological disease. *Journal of Neuroscience Methods*, *331*, 108484. <https://doi.org/10.1016/j.jneumeth.2019.108484>

- Pontikis, C. C., Cella, C. V., Parihar, N., Lim, M. J., Chakrabarti, S., Mitchison, H. M., Mobley, W. C., Rezaie, P., Pearce, D. A., & Cooper, J. D. (2004). Late onset neurodegeneration in the *Cln3^{-/-}* mouse model of juvenile neuronal ceroid lipofuscinosis is preceded by low level glial activation. *Brain Research*, *1023*, 231–242. <https://doi.org/10.1016/j.brainres.2004.07.030>
- Ranta, S., Savukoski, M., Santavuori, P., & Haltia, M. (2001). Studies of homogenous populations: CLN5 and CLN8. In K. E. Wisniewski & G. Zhong (Eds.), *Batten disease: Diagnosis, treatment, and research* (pp. 123–140). Academic Press. [https://doi.org/10.1016/S0065-2660\(01\)45007-3](https://doi.org/10.1016/S0065-2660(01)45007-3)
- Rietdorf, K., Coode, E. E., Schulz, A., Wibbeler, E., Bootman, M. D., & Ostergaard, J. R. (2020). Cardiac pathology in neuronal ceroid lipofuscinoses (NCL): More than a mere co-morbidity. *Biochimica et Biophysica Acta—Molecular Basis of Disease*, *1866*, 165643. <https://doi.org/10.1016/j.bbadis.2019.165643>
- Sanders, D. N., Kanazono, S., Wininger, F. A., Whiting, R. E. H., Flournoy, C. A., Coates, J. R., Castaner, L. J., O'Brien, D. P., & Katz, M. L. (2011). A reversal learning task detects cognitive deficits in a Dachshund model of late-infantile neuronal ceroid lipofuscinosis. *Genes, Brain and Behavior*, *10*, 798–804. <https://doi.org/10.1111/j.1601-183X.2011.00718.x>
- Santavuori, P., Vanhanen, S. L., & Autti, T. (2001). Clinical and neuroradiological diagnostic aspects of neuronal ceroid lipofuscinoses disorders. *European Journal of Paediatric Neurology*, *5*, 157–161. <https://doi.org/10.1053/ejpn.2000.0454>
- Schaefer, J., van derGiessen, L. J., Klees, C., Jacobs, E. H., Sieverdink, S., Dremmen, M. H. G., Spoor, J. K. H., van derPloeg, A. T., vanden Hout, J. M. P., & Huidekoper, H. H. (2021). Presymptomatic treatment of classic late-infantile neuronal ceroid lipofuscinosis with cerliponase alfa. *Orphanet Journal of Rare Diseases*, *16*, 1–9. <https://doi.org/10.1186/s13023-021-01858-6>
- Schlaepfer, I. R., & Joshi, M. (2020). CPT1A-mediated fat oxidation, mechanisms, and therapeutic potential. *Endocrinology (United States)*, *161*, 1–14. <https://doi.org/10.1210/endo/bqz046>
- Schmiedt, M. L., Bessa, C., Heine, C., Ribeiro, M. G., Jalanko, A., & Kyttälä, A. (2010). The neuronal ceroid lipofuscinosis protein CLN5: New insights into cellular maturation, transport, and consequences of mutations. *Human Mutation*, *31*, 356–365. <https://doi.org/10.1002/humu.21195>
- Schmutz, I., Jagannathan, V., Bartenschlager, F., Stein, V. M., Gruber, A. D., Leeb, T., & Katz, M. L. (2019). ATP13A2 missense variant in Australian Cattle Dogs with late onset neuronal ceroid lipofuscinosis. *Molecular Genetics and Metabolism*, *127*, 95–106. <https://doi.org/10.1016/j.ymgme.2018.11.015>
- Schulz, A., Ajayi, T., Specchio, N., deLos Reyes, E., Gissen, P., Ballon, D., Dyke, J. P., Cahan, H., Slasor, P., Jacoby, D., & Kohlschütter, A. (2018). Study of intraventricular Cerliponase Alfa for CLN2 Disease. *New England Journal of Medicine*, *378*, 1898–1907. <https://doi.org/10.1056/nejmoa1712649>
- Shyng, C., & Sands, M. S. (2014). Astrocytosis in infantile neuronal ceroid lipofuscinosis: Friend or foe? *Biochemical Society Transactions*, *42*, 1282–1285. <https://doi.org/10.1042/BST20140188>
- Siakotos, A. N., Hutchins, G. D., Farlow, M. R., & Katz, M. L. (2001). Assessment of dietary therapies in a canine model of Batten disease. *European Journal of Paediatric Neurology*, *5*, 151–156. <https://doi.org/10.1053/ejpn.2000.0453>
- Simonati, A., Williams, R. E., Nardocci, N., Laine, M., Battini, R., Schulz, A., Garavaglia, B., Moro, F., Pezzini, F., & Santorelli, F. M. (2017). Phenotype and natural history of variant late infantile ceroid-lipofuscinosis 5. *Developmental Medicine & Child Neurology*, *59*, 815–821. <https://doi.org/10.1111/dmcn.13473>
- Skerritt, G. (Ed.) (2018) *King's applied anatomy of the central nervous system of domestic mammals* (2nd ed.). John Wiley & Sons, Inc.
- Stephenson, J., Nutma, E., van derValk, P., & Amor, S. (2018). Inflammation in CNS neurodegenerative diseases. *Immunology*, *154*, 204–219. <https://doi.org/10.1111/imm.12922>
- Topál, J., Román, V., & Turcsán, B. (2019). The dog (*Canis familiaris*) as a translational model of autism: It is high time we move from promise to reality. *Wiley Interdisciplinary Reviews: Cognitive Science*, *10*, 1–11. <https://doi.org/10.1002/wcs.1495>
- Tracy, C. J., Whiting, R. E. H., Pearce, J. W., Williamson, B. G., Vansteenkiste, D. P., Gillespie, L. E., Castaner, L. J., Bryan, J. N., Coates, J. R., Jensen, C. A., & Katz, M. L. (2016). Intravitreal implantation of TPP1-transduced stem cells delays retinal degeneration in canine CLN2 neuronal ceroid lipofuscinosis. *Experimental Eye Research*, *152*, 77–87. <https://doi.org/10.1016/j.exer.2016.09.003>
- Tyynelä, J., Cooper, J. D., Khan, M. N., Shemilts, S. J. A., & Haltia, M. (2004). Hippocampal pathology in the human neuronal ceroid-lipofuscinoses: Distinct patterns of storage deposition, neurodegeneration and glial activation. *Brain pathology (Zurich, Switzerland)*, *14*, 349–357. <https://doi.org/10.1111/j.1750-3639.2004.tb00077.x>
- Tyynelä, J., Suopanki, J., Santavuori, P., Baumann, M., & Haltia, M. (1997). Variant late infantile neuronal ceroid-lipofuscinosis. *Journal of Neuropathology and Experimental Neurology*, *56*, 369–375. <https://doi.org/10.1097/00005072-199704000-00005>
- Villani, N. A., Bullock, G., Michaels, J. R., Yamato, O., O'Brien, D. P., Mhlanga-Mutagadura, T., Johnson, G. S., & Katz, M. L. (2019). A mixed breed dog with neuronal ceroid lipofuscinosis is homozygous for a CLN5 nonsense mutation previously identified in Border Collies and Australian Cattle Dogs. *Molecular Genetics and Metabolism*, *127*, 107–115. <https://doi.org/10.1016/j.ymgme.2019.04.003>
- Villela, N. R., do Nascimento, P. Jr, Carvalho, L. R., & Teixeira, A. (2005). Effects of dexmedetomidine on renal system and on vasopressin plasma levels. Experimental study in dogs. *Revista Brasileira de Anestesiologia*, *55*, 429–440. <https://doi.org/10.1590/s0034-70942005000400007>
- vonDehn, B. (2014). Pediatric clinical pathology. veterinary clinics of North America. *Small Animal Practice*, *44*, 205–219. <https://doi.org/10.1016/j.cvsm.2013.10.003>
- Vuilleminot, B. R., Kennedy, D., Cooper, J. D., Wong, A. M. S., Sri, S., Doeleman, T., Katz, M. L., Coates, J. R., Johnson, G. C., Reed, R. P., Adams, E. L., Butt, M. T., Musson, D. G., Henshaw, J., Keve, S., Cahayag, R., Tsuruda, L. S., & O'Neill, C. A. (2015). Non-clinical evaluation of CNS-administered TPP1 enzyme replacement in canine CLN2 neuronal ceroid lipofuscinosis. *Molecular Genetics and Metabolism*, *114*, 281–293. <https://doi.org/10.1016/j.ymgme.2014.09.004>
- Whiting, R. E. H., Narfström, K., Yao, G., Pearce, J. W., Coates, J. R., Castaner, L. J., Jensen, C. A., Dougherty, B. N., Vuilleminot, B. R., Kennedy, D., O'Neill, C. A., & Katz, M. L. (2014). Enzyme replacement therapy delays pupillary light reflex deficits in a canine model of late infantile neuronal ceroid lipofuscinosis. *Experimental Eye Research*, *125*, 164–172. <https://doi.org/10.1016/j.exer.2014.06.008>
- Whiting, R. E. H., Jensen, C. A., Pearce, J. W., Gillespie, L. E., Bristow, D. E., & Katz, M. L. (2016). Intracerebroventricular gene therapy that delays neurological disease progression is associated with selective preservation of retinal ganglion cells in a canine model of CLN2

- disease. *Experimental Eye Research*, 146, 276–282. <https://doi.org/10.1016/j.exer.2016.03.023>
- Wright-Jin, E. C., & Gutmann, D. H. (2019). Microglia as dynamic cellular mediators of brain function. *Trends in Molecular Medicine*, 25, 967–979. <https://doi.org/10.1016/j.molmed.2019.08.013>
- Xin, W., Mullen, T. E., Kiely, R., Min, J., Feng, X., Cao, Y., O'Malley, L., Shen, Y., Chu-Shore, C., Mole, S. E., Goebel, H. H., & Sims, K. (2010). CLN5 mutations are frequent in juvenile and late-onset non-Finnish patients with NCL. *Neurology*, 74, 565–571. <https://doi.org/10.1212/WNL.0b013e3181cff70d>
- Xiong, J., & Kielian, T. (2013). Microglia in juvenile neuronal ceroid lipofuscinosis are primed toward a pro-inflammatory phenotype. *Journal of Neurochemistry*, 127, 245–258. <https://doi.org/10.1111/jnc.12385>

SUPPORTING INFORMATION

Additional supporting information may be found in the online version of the article at the publisher's website.

How to cite this article: Meiman, E. J., Kick, G. R., Jensen, C. A., Coates, J. R., & Katz, M. L. (2022). Characterization of neurological disease progression in a canine model of CLN5 neuronal ceroid lipofuscinosis. *Developmental Neurobiology*, 82, 326–344. <https://doi.org/10.1002/dneu.22878>